



UNIVERSITAT DE
BARCELONA

Treball Final de Grau

Study of the sensitivity of Fire Dynamics Simulator and its applicability in different fields of fire research

Guillem Larrubia Torres

June 2024

Aquesta obra està subjecta a la llicència de:
Reconeixement–NoComercial–SenseObraDerivada



<http://creativecommons.org/licenses/by-nc-nd/3.0/es/>

*Res no neix ni és destruït, sinó que hi ha barreja
de les coses que són.*

Anaxàgores

En primer lloc m'agradaria expressar l'agraïment al meu tutor, el Dr. Roger Bingué Tomàs, pel seu suport durant l'elaboració d'aquest treball però, especialment pel guiatge i la confiança que m'ha ofert aquests darrers anys.

En segon lloc als companys de Bombers de Barcelona, per les facilitats que m'han ofert a l'hora de cursar aquests estudis, per l'interès mostrat en el seu progrés així com l'ajuda per a dur a terme el Treball Final de Grau.

En tercer lloc als meus fills, per la curiositat infinita pels gargots, símbols i lletres estranyes que tant temps els han robat. Als meus pares, per sempre preguntar.

I com sempre, a la Carmen , per la seva paciència sense fi i el suport en els moments més complicats i foscos d'aquest camí.

CONTENTS

SUMMARY	I
RESUM	III
SUSTAINABLE DEVELOPMENT GOALS	V
1. INTRODUCTION	1
1.1. Fire behavior	2
1.1.1. Fundamentals of combustion	3
1.1.2. Pyrolysis	4
1.1.3. Ignition and flame	6
1.1.3.1. Flash Point	7
1.1.3.2. Ignition Point	7
1.1.3.3. Auto-inflammation point	7
1.1.4. Heat Release Rate	8
1.1.5. Fire stages and design fires	9
2. OBJECTIVES	14
3. NUMERICAL FIRE MODELING	15
3.1. Fire Dynamics Simulator	16
3.1.1. Fundamental conservation equations	17
3.1.2. The low Mach-number approach	17
3.1.3. Turbulence model	19
3.1.3.1. Direct Numerical Simulation	20
3.1.3.2. Large-Eddy Simulation model	20
3.1.3.3. Reynolds-Averaged Navier-Stokes model	22
3.1.4. Combustion model	23
3.1.5. Design fire	26
3.1.5.1. Burner fire	26
3.1.5.2. Material defined fire	26
3.1.6. Energy equation	26
4. CONDUCTED SIMULATIONS	29
4.1. Scale Model Simulations	29

4.1.1.	Bidirectional fire	30
4.1.2.	Unidirectional fire	31
4.1.3.	Pulsating smoke	32
4.1.4.	Backdraft	32
4.1.5.	Simulation Parameters	33
4.1.5.1.	Grid size	33
4.1.5.2.	Ignition process	33
4.2.	Chemical engineering Laboratory Simulations	34
4.2.1.	Simulation Parameters	35
4.2.2.	Output Parameters	36
4.2.2.1.	CO concentration	36
4.2.2.2.	Smoke layer height	37
4.2.2.3.	Ceiling temperature	37
5.	RESULTS	38
5.1.	Scale model simulations	38
5.1.1.	Ventilation behaviour simulations	38
5.1.2.	Backdraft simulation	41
5.2.	Chemical engineering laboratory simulations	43
5.2.1.	CO concentrations	43
5.2.2.	Smoke layer height	45
5.2.3.	Ceiling temperature	46
6.	CONCLUSIONS	51
2.	REFERENCES AND NOTES	53
3.	ACRONYMS	54
	APPENDICES	55
4.	APPENDIX 1: FDS CODE	57
6.1.	Backdraft simulation	57
6.2.	Ventilation patterns simulations	61
6.3.	Chemical engineering laboratory Simulations	66

SUMMARY

The evolution of computer technology has allowed for the development of computer simulation tools in the field of fluid dynamics (CFD), enabling the exploration of various aspects of engineering with a precision in calculation that would otherwise be unattainable.

Fire engineering, or fire protection engineering, involves analyzing the behavior of fires and designing solutions intended to be applied to buildings and industries to protect people and structures from the effects of fire. The use of CFD tools is well established in engineering fields such as chemical, mechanical, or aeronautical engineering. However, in fire engineering, the complexity of the accidental fire phenomenon, as well as the degree of uncertainty it presents, makes its application more challenging and the acceptance of justifications based on simulations is lower than it would be in other fields.

The Fire Dynamics Simulator (FDS), developed by the National Institute of Standards and Technology (NIST) of the United States, is the reference software for fire simulation in the field of fire engineering. It is commonly used to justify design solutions for fire protection that differ from those specified in fire regulations. It has also been used forensically for fire reconstruction as well as in various areas of fire science research.

This work was intended to study the various phenomena that explain the behavior of compartment fires and to relate the physical and chemical principles governing them to the models and simplifications used by FDS software in order to evaluate the capabilities and limitations of this software. Simulations were conducted in different scenarios to study the program's ability to reproduce some phenomena of interest, as well as to analyze the sensitivity of the results to design decisions in characterizing input variables.

FDS presented strong capabilities in representing fire phenomena related to the movement of smoke and hot gases, even in rapidly changing scenarios. However, when input parameters such as grid size or fire location were slightly changed, significant variations in output emerged, which could mislead the interpretation of the results.

Keywords: Fire engineering, computational fluid dynamics, fire behavior

RESUM

L'evolució de la tecnologia informàtica ha permès el desenvolupament d'eines de simulació per ordinador en el camp de la dinàmica de fluids computacional (CFD) permetent abordar aspectes de diverses branques de l'enginyeria amb una precisió en el càlcul que, d'altra banda, seria inviable d'obtenir.

L'enginyeria del foc, o enginyeria de protecció contra incendis, s'ocupa d'analitzar el comportament dels incendis i de dissenyar solucions destinades a ser aplicades a edificis i indústries per tal de protegir les persones i les construccions dels efectes del foc. L'ús d'eines CFD està ben consolidat en àmbits de l'enginyeria com poden ser les enginyeries química, mecànica o aeronàutica. En l'enginyeria del foc, en canvi, la complexitat del fenomen de l'incendi accidental, així com el grau d'incertesa que aquest presenta, fa que la seva aplicació presenti més dificultats i l'acceptació de justificacions basades en simulacions sigui menor del que seria en d'altres àmbits.

El Fire Dynamics Simulator (FDS), desenvolupat per l'Institut Nacional d'Estàndards i Tecnologia dels Estats Units (NIST), és el programari de referència per a la simulació d'incendis al món de l'enginyeria del foc. S'utilitza habitualment per justificar solucions constructives i de disseny d'instal·lacions de protecció contra incendis diferents de les que es recullen en les normatives d'aquest àmbit, així com a nivell forense per a la reconstrucció d'incendis i en diferents àmbits de recerca de la ciència del foc.

El present treball va néixer amb l'objectiu d'estudiar els diversos fenòmens que expliquen el comportament dels incendis en interiors i relacionar-ne els fonaments físics i químics que els regeixen amb els models utilitzats pel programari, amb la finalitat d'avaluar-ne les seves capacitats i limitacions. Simulacions en diferents escenaris han estat realitzades per tal d'estudiar la capacitat del programa de reproduir alguns fenòmens d'interès, així com per analitzar la sensibilitat que els resultats presenten en funció de les decisions de disseny en caracteritzar les variables d'entrada.

El programa ha mostrat bones capacitats en la simulació de fenòmens d'incendis en interiors associats als patrons de ventilació, fins i tot en escenaris amb canvis eren sobtats. No obstant, en modificar lleugerament paràmetres d'entrada com la mida de la graella o la ubicació relativa de l'incendi, han sorgit diferències en els resultats que podrien dur a mal interpretar-los.

Paraules clau: Enginyeria del foc, dinàmica de fluids computacional, comportament del foc

SUSTAINABLE DEVELOPMENT GOALS

L'estudi de les eines de simulació per computador té l'objectiu final de poder complementar, i, en última instància, substituir l'experimentació en diversos àmbits de la ciència i l'enginyeria. La ciència del foc, com qualsevol branca de la ciència, té una gran necessitat de recollir dades experimentals que permetin construir el coneixement necessari per a poder predir l'origen, desenvolupament i conseqüències d'un incendi i així poder-ne prevenir i reduir l'impacte que tenen a la societat. En aquest sentit, el present treball, que es centra en l'ús i l'estudi del programari Fire Dynamics Simulator, encaixa amb diversos dels objectius recollits a la guia de l'Organització de Nacions Unides. Especialment rellevants s'ha considerat l'encaix els objectius número 3: salut i benestar i l'objectiu 11: ciutats inclusives, segures, resilents i sostenibles.

Objectiu 3: Salut i Benestar

L'objectiu últim en la ciència i enginyeria del foc és la protecció de la salut i la integritat de les persones mitjançant la prevenció d'incendis així com la protecció quan han ocorregut i l'actuació per a limitar-ne les conseqüències. La recerca en aquest camp permetrà, en un futur, adoptar solucions més efectives i més econòmiques, i per tant, a l'abast de més persones.

Objectiu 11: Ciutats inclusives, segures, resilents i sostenibles

Lamentablement, els darrers anys han ocorregut diversos incendis greus amb un elevat nombre de víctimes mortals que s'han produït en condicions poc estudiades des del punt de vista científic i, sovint, a les zones més densament habitades dels països o ciutats d'arreu. Alguns exemples recents en són els incendis forestals de Chile o Grècia i els incendis dels edificis de València o la Torre Grenfell de Londres.

L'estudi de les eines de simulació d'incendis aplicades a escenaris que fins ara són desconeguts i difícilment reproduïbles experimentalment, permetrà que les normatives reguladores de l'edificació i urbanisme s'adaptin i actualitzin per tal de prevenir aquestes situacions

1. INTRODUCTION

The discovery of fire in human history is arguably the most influential moment in human history. From providing warmth and protection to becoming a central element in the Industrial Revolution, the control of such a powerful phenomenon has become a central element in the development of human society. In addition to its importance in our progress, fire possesses a potential for destruction that has also had a significant effect on the way societies organize their cities, industries, and ways of living. From wildfires to the devastation of entire cities, the power of fire has also taken thousands of lives and countless resources throughout the ages.

From the theories of the ancient Greek philosophers regarding the basic four elements to the alchemist's notion of phlogiston, and culminating in the studies of Antoine Lavoisier on combustion, scientists have attempted to comprehend the nature and behavior of fire. The progression of computer science and technology within the past two decades has had a major impact in the evolution of Computational Fluid Dynamics (CFD) and its use in tackling complex problems in different fields of engineering, from aerodynamics to virtually every field in engineering involving fluid motion. Fire Safety Engineering is one of the fields that has benefited greatly in the CFD. It is now possible to develop models that can predict smoke movement and its effects in people's evacuation from buildings, as well as study the safety of structures involved in fires.

Most European countries have their own fire safety regulations regarding the measures that must be taken when legalizing new buildings, industries, or activities. While these regulations include explicit measures that cover every aspect of the projects, most of them also allow for the use of alternative solutions as long as they provide equivalent safety levels to the legal requirements. It is in this field where the development of the software Fire Dynamics Simulator (FDS) has become the primary tool of choice for many engineers to simulate fires and predict their behavior, as well as the effects they may have on structural safety, evacuation conditions, firefighter operations, and more. Furthermore, in fire investigation, FDS has been used to

reconstruct and analyze fire incidents to support physical evidence or to assess the credibility of witnesses and experts.

While FDS is a sophisticated tool which has surpassed other more limited fire modeling techniques, the accidental nature of fire and the complexity and diversity of phenomena that occur in a compartment fire make it very difficult to predict with accuracy the various data of interest, such as temperature distribution, toxic concentrations, or visibility conditions. It is not only near to impossible to model accidental fires with a high level of accuracy, but also there is a need to take various simplifications in order to make it computationally viable. Additionally, input choices have to be made by the user when modeling the fire and simplifications are needed for reproducing geometries or compound material properties. Assumptions about human behavior also need to be considered.

1.1. FIRE BEHAVIOR

While fire is purely the result of chemical processes, fire behavior and mode of combustion is more dependent on physical conditions and environment rather than the chemical nature of the reactants. This can be exemplified by considering the flammability of wheat flour: while a pile of flour undergoes a relatively slow combustion, a cloud of flour dust may be a highly explosive mixture.

To comprehend the behavior of compartment fires we need to examine the interactions between fuel and its environment concerning mass and heat transfer processes. Figure 1.1 illustrates these relations.

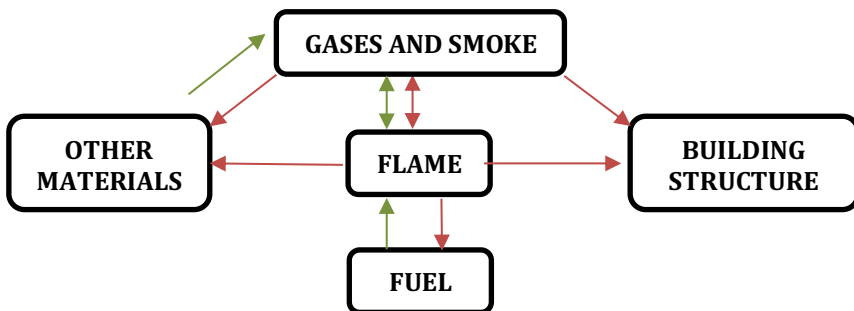
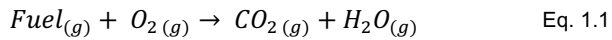


Figure 1.1. Heat and mass flow relations between fuel and its surroundings. Green arrows represent mass flux and red arrows represent heat flux

The understanding of fire behavior not only requires knowledge of chemistry, but also other engineering fields such as fluid dynamics and heat and mass transfer (1). Furthermore, the dependence between the chemical reaction and its surroundings can be very complex and highly nonlinear (2).

1.1.1. Fundamentals of combustion

This chapter aims to be an overview of combustion in accidental fire scenarios, where the predominant fuels are carbon-based materials in solid or liquid phases, with oxygen from air as the primary oxidizer.



Combustion is a chemical reaction involving some kind of fuel, typically composed of molecules containing different combinations of carbon, hydrogen, and oxygen atoms. Other common fuels may also contain other atoms like nitrogen or chlorine. These two reactants, fuel and oxygen, react to produce different products depending on the nature of the reactants and the conditions under which the reaction takes place. Among the products, excess fuel and oxygen may be included as well as the portion of air, mostly nitrogen, that is transported with no change. The reaction takes place with the release of heat, and usually with the presence of a flame, which is the visible portion of the volume where the oxidation is taking place.

It is common to differentiate between complete and incomplete combustion processes. For fuels in the form of $\text{C}_x\text{H}_y\text{O}_z$, a complete combustion will produce CO_2 and H_2O , which are the products in their most stable form. However, complete combustions are rare, and the most usual situation is some deviation from completeness. On the other hand, incomplete combustion results in additional products such as CO , H_2 and soot. For fuels containing chlorine or nitrogen, incomplete combustion will produce HCN and HCl (2), and while these products may have an impact on toxicity, the principal toxic species is CO , which is produced in all fires. The effect of incompleteness in fire behavior is especially important when considering factors such as toxicity and visibility. Additionally, the incomplete products carried in the smoke layer can still act as fuel, potentially igniting in distant locations from the fire origin.

1.1.2. Pyrolysis

Flame is a phenomenon that occurs in a gas phase; thus, combustion of solid and liquid fuels requires physical and chemical transformations to gaseous form. The process of conversion to gaseous phase is different for liquid and solid fuels. While most liquid fuels undergo a simple evaporation process due to boiling, virtually all solids, with very few exceptions, experience a series of decomposition processes, known as pyrolysis, to produce molecules light enough to volatilize from the surface of the solid and react in gaseous form. The process of pyrolysis requires more energy than evaporation, this is the reason why the surface of burning solids will be at higher temperatures than liquid fuels. Once the ignition has occurred, this energy is provided from the reaction itself, generating a mass flux of volatiles from the solid fuel that sustains the reaction while there is sufficient oxygen available.

Most solid fuels consist of natural or man-made polymeric materials. Examples include cellulose present in wood or cotton, as well as polyethylene or polypropylene present in many household items. The varying degrees of cross-linked structure in different polymeric materials will lead to different pyrolysis products, from hydrogen to molecules which are volatile only at high temperatures due to their high molecular weight but will condense as they cool down.

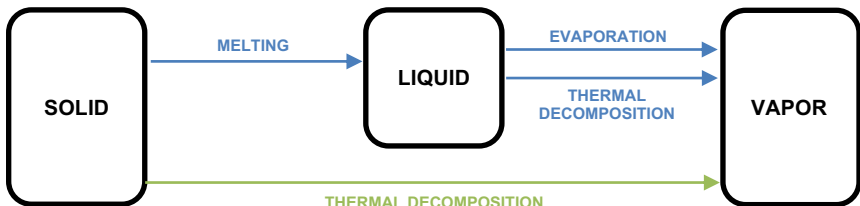


Figure 1.2 Different modes of flammable vapor production

Different pyrolysis processes may lead to different fire behaviors. In highly cross-linked structures, volatilization typically will take place without melting, and decomposition proceeding directly from the solid phase. Additionally, flammability tends to decrease due to the formation of non-volatile carbon residue or char, which can account for up to 60% in phenolic resins. Alternatively, thermoplastics typically melt or soften before producing volatiles.

Depending on their monomer structure, some thermoplastics, such as PMMA, break their chains at specific points defined by the monomer structure. These molecules decrease slowly

and tend to soften instead of melting. In contrast, other polymers, like polyethylene, break at random points in the chain, resulting in a rapid decrease of the molecular weight that facilitates easy melting. The melting of polymeric materials, as seen in wall coverings for example, can participate in fire spread due to falling droplets that may ignite when they are deposited on the surface of other flammable materials.

It should be noted that the complexity of pyrolysis involves the diverse nature of the products of decomposition that may be different in changing conditions, but also because commercial polymers contain additives which will have an impact in the physical processes of phase change. Geometric factors also have an influence in heat transfer which also will modify the rate of pyrolysis. Furthermore, wood and some other materials can absorb moisture from the air, and this may have an impact both in the physical and chemical properties of the fuel. (3)

This complexity makes it practical to describe fire behavior of solid materials in terms of their composition, reactivity, and rate of formation. The decomposition can be idealized assuming a first order kinetic reaction in the form of:

$$\frac{dm}{dt} = -k' \cdot m \quad \text{Eq. 1.2}$$

Where k' is the kinetic rate constant of reaction that can be expressed using an Arrhenius type relation, which remarks the temperature dependence of pyrolysis. (1)

$$k' = A \cdot e^{\frac{-E_a}{R \cdot T}} \quad \text{Eq. 1.3}$$

The rate of formation can be measured using thermogravimetric analysis (TGA) by analyzing the mass loss rate and its dependence with temperature. It is possible also, for small samples, to couple the TGA with a mass spectrometer to identify the products of pyrolysis. The nature of the volatiles will determine the quantity of soot produced. Soot is a complex mixture of carbon-based particles that are produced in incomplete combustions and is the primary factor controlling radiation to the surroundings, as well as the quantity and opacity of smoke released.

(1)

1.1.3. Ignition and flame

It is necessary to differentiate two different regimes in which burning of fuel can take place in order to be able to describe the combustion process. The first regime is characterized by the pre-ignition mixture between the fuel and the oxidizer, in our case air. The second regime occurs when the air becomes entrapped in flow movement of the fuel, leading to a flammable mixture only in certain areas of the fuel mass flow. These two regimes generate two different categories of flames: premixed flames and diffusion flames. The vast majority of accidental fires involving liquid and solid fuels are characterized by diffusion flames.

The burning rate in diffusion flames depends on the rate at which the gaseous fuel is supplied. In the case of liquid and solid fuels, the mass flow rate of volatiles depends directly on the heat transfer from the flame. The rate of burning, whether from liquid or solid fuels, can be expressed as the ratio between the net heat flux to the fuel and the heat required to produce the gaseous form of the fuel.

$$\dot{m}'' = \frac{\dot{Q}''_F - \dot{Q}''_L}{L_v} \quad \text{Eq. 1.4}$$

Where the numerator represents the difference between the heat transferred from the flame to the fuel and the heat losses from the fuel to the surroundings, expressed in kW/m², and L_v is the heat of vaporization of the fuel, in kJ/kg. For liquids, L_v is simply the enthalpy of evaporation, for solids is not a constant property as it depends on geometry, char formation and other parameters. (2) As expressed in the previous equation, heat transfer processes are key in order to determine the mass flow rate from the fuel to the flame.

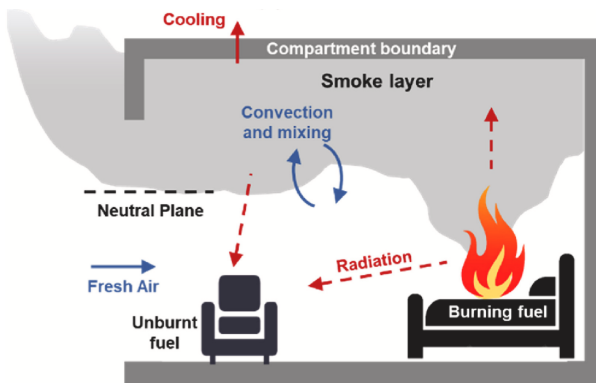


Figure 1.3 Typical representation of a compartment fire

(Source: Tianhang Zhang et al, Real-time forecast of compartment fire and flashover based on deep learning. Fire Safety Journal.)

There are three different temperatures at which ignition can occur and present different behavior; these are the flash point, the ignition point and the auto-inflammation point. These temperatures are characteristic of the material and depend on composition and physical conditions.

1.1.3.1. Flash Point

The flash point is the lowest temperature at which a fuel can ignite if an ignition source, such as a flame or a spark, is applied near the fuel surface. At this temperature, if the ignition source is removed, the fuel will not produce enough flammable vapors to sustain combustion.

1.1.3.2. Ignition Point

The ignition point is a temperature slightly above the flash point and corresponds to the temperature at which combustion will be sustained when the ignition source is removed, but it still necessary in order to initiate ignition. This is the most common form of ignition in both accidental and non-accidental fires, it is known as piloted ignition.

1.1.3.3. Auto-inflammation point

The auto-inflammation point is a temperature, usually significantly higher than the flash and ignition points, at which the vapors of the fuel will ignite without an external source of ignition.

Reference temperatures for pure ethanol are showed in the table below:

Entry	Reference Temperature	Temperature Value [°C]
1	Flash Point	13
2	Ignition Point	15-17
3	Autoinflammation Point	365

Table 1. Reference ignition temperatures for pure ethanol

1.1.4. Heat Release Rate

The factor which has the most impact in the development of a compartment fire as well as its consequences, is the rate at which the energy is released, usually named heat release rate (HRR). Heat release rate have more impact in the fire behavior than the total amount of energy released (1). Strictly, the heat release rate can be defined by the following expression:

$$\dot{Q}_c = \chi \cdot \dot{m}'' \cdot A_f \cdot \Delta H_c \quad \text{Eq. 1.5}$$

Where χ represents the degree of incompleteness of the reaction, and it's a value between 0 and 1. A_f is the surface of the fuel (m^2) and ΔH_c is the heat of combustion of the volatiles or the gas phase of the fuel, when oxidized completely. Most compartment fires are incomplete process, thus most of the time χ will be less than 1. Assuming a two-step process for a standard combustion: one step to form CO and H_2O and another for CO_2 formation, the heat of combustion could be calculated using the heats of formation and Hess's law. However, due to the unknown number and nature of products in incomplete combustions, this is not appropriate.

It can be observed that the heat of combustion remains relatively constant when expressed in relation to the amount of oxygen or air consumed. For most fuels this value is nearly constant at approximately 13kJ/g of oxygen, or 3 kJ/g of air. Utilizing this principle, the heat release rate can be estimated if the inflow of air is known or can be calculated.

Alternatively, experimental methods are used to determine the heat release rate (\dot{Q}_c) which is a crucial information for many engineering purposes. The most used instrument is the cone calorimeter, which operates on the basis that the amount of heat released in combustion is constant in relation to oxygen consumed.

The cone calorimeter is capable of calculating the effective heat of combustion by analyzing the flow of gaseous products, determining the amount of oxygen consumed, and measuring the mass loss of the sample. This measurement provides a value for the total heat released. However, in fire engineering, the total heat released by the fire is of secondary importance compared to the rate at which heat is released. Most fire engineering applications such as evacuation routes design, preventing fire spread, or fire suppression are constrained by time frames in which the design needs to operate. Therefore, it is valuable to determine instantaneous values of these parameters at different times during the test. (1)

Many data in heat release rate are published in various sources, providing values for a wide range of materials and specific products. While this data is highly valuable for engineers, it should be used as guide, material composition, variations in geometry and changes in test conditions for similar items can all influence results.

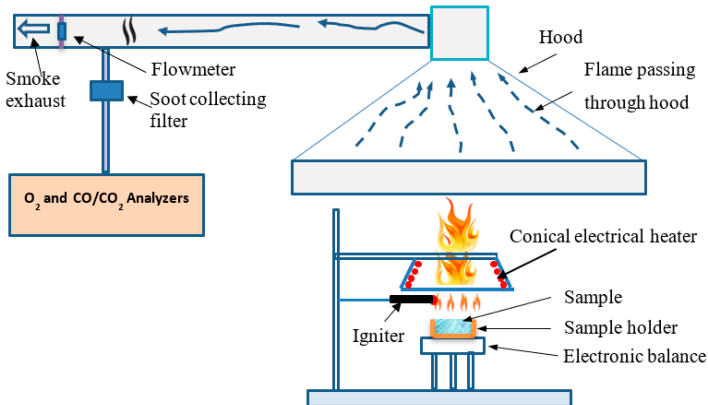


Figure 1.4. Cone calorimeter scheme

(Source: sanjay pareek – journal of material sciences and engineering, d.o.i: 10.17265/2161-6221/2017.3-4.005)

Although the test presumes a complete combustion, and the heat of combustion used is an average value, the assumption is that the error on the rate of heat release of monoxide and soot yield will be less than 5%. (8)

The two approaches described above for determining the HRR, analytical and experimental, can be employed when the scenario to be simulated is well known and materials bound to initiate a fire are well defined, both in their nature and quantity. However, when there is limited knowledge of the fuel involved, an alternative approach based on the type of activity or occupancy might be used. This latter approach relies on statistics that are reflected in fire regulations and are not within the scope of this dissertation.

1.1.5. Fire stages and design fires

Compartment fires can be described using five idealized stages that relate the variation of temperature in the room with respect to time. The stages described might not be present in all situations, while all fires will have an ignition phase, not all of them will grow and others will be

suppressed before arriving to the final theoretical stages. For a fire without fire control, the typical growth stages are (4):

1. Ignition
2. Growth
3. Flashover
4. Fully developed fire
5. Decay

Ignition: Ignition is the period where fire begins. This process can be in one of two ways: piloted or spontaneous ignition. Piloted ignition is the process where the combustion reaction is initiated by an external energy source such as a match or a spark. Spontaneous ignition, on the other hand, is when the fuel is heated enough to arrive at his auto-ignition temperature.

Growth: After ignition fire will begin to grow, initially, without dependence on the compartment. The type of fuel will determine the initial rate of growth. After these initial moments, interaction with the surroundings will impact the growth behavior. The fire can be described in terms of the heat release rate and can be classified based on different growth velocities.

Flashover: The general definition of the flashover phenomena is that it represents the transition from a growing fire to a fully developed fire, where all the fuel present in the room is involved in the fire. Flashover is typically defined as the stage where a specific temperature range is reached, generally between 500°C and 600°C, at which point all materials in the enclosure have undergone pyrolysis and the temperature of the flammable vapors is sufficiently high to ignite.

Fully developed fire: This stage is where the heat release rate is at its maximum. The energy radiated to the materials present in the compartment leads to more pyrolysis products than can be burned due to the limited oxygen available in the room. Unburned products will burn upon mixing with fresh air, usually outside of the compartment when a vent is opened, for example when a window breaks. At this stage the fire is not controlled by fuel anymore, but rather by ventilation.

Decay stage: As the fuel exhausts, the heat release rate also declines and, usually, fire becomes fuel controlled again.

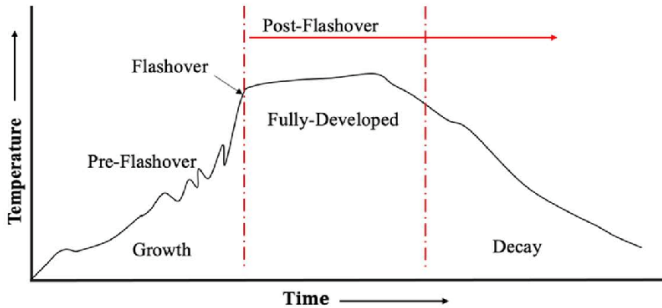


Figure 1.5. Stages of fire in a compartment

(Source: Aatif Ali Khan – Fire safety journal, d.o.i: doi.org/10.1016/j.firesaf.2021.103367)

Fire safety objectives included in building regulations primarily aim to ensure the safety of occupants by minimizing the likelihood for a fire to take place and by limiting its growth and spread capabilities, thus facilitating the evacuation of the building. Additionally, another primary objective is to prevent the structural collapse due to damage caused by fire. These two objectives have very different time frames, a few minutes in the case of evacuation to potentially several hours for structural safety. Consequently, different approaches are necessary when trying to predict the effects of a hypothetical fire. Therefore, the design fire may present different characteristics depending on the objective to be achieved.

Design fires are characterized by curves that describe the evolution of a particular parameter of interest of the fire, typically temperature or heat release rate, over time. The simplest approach to define a fire curve is to represent three different phases: a growth phase, a steady phase and a decay phase.

Growth phase: The growth phase represents the accelerating development of the fire in the early stages. The most usual approach, mathematically, is to assume that the rate at which the heat is released grows as the square of time. This is called the t-squared fire, and it is possible to simulate different growth velocities by multiplying the square of time by a growth factor, α . Thus, the heat release rate in this phase can be expressed as follows:

$$\dot{Q} = \alpha \cdot t^2$$

Eq. 1.6

Different regulations as well and literature suggest various growth parameters to define the fire curves depending on the expected growth rate and relate each rate with different kind of fuels.

Entry	Fire growth rate	Value of α [kW/s ²]
1	Slow	0,00293
2	Medium	0,01172
3	Fast	0,0469
4	Ultra-fast	0,1876

Table 2. Fire growth parameters specified in NFPA 92b

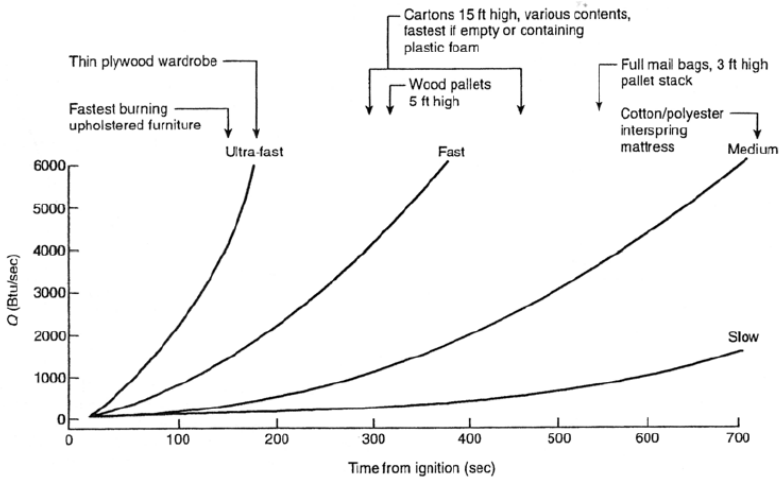


Figure 1.6. Fire growth curves specified in NFPA 92b

Steady phase: Depending on the availability of oxygen, the fire will be either fuel-controlled or ventilation-controlled. Consequently, the growth phase will lead to one of these two scenarios. A steady phase will follow the growth phase, but its duration and the heat release rate at which the phase remains, will depend on the factors that characterize the growth phase.

Decay phase: The decay phase will usually have very little to no relevance in most engineering applications because the effects of the fire on people and structures occur during

the growth and steady phases. Additionally, the fire service is expected to intervene in the first 30 minutes of the fire; in Barcelona this time is reduced to 10 minutes from the first call. While the fire simulation tools can represent different forms of fire suppression, adding another layer of complexity may result in a much less accurate outcome.

2. OBJECTIVES

The objectives of the present work can be categorized into two groups.

The first group of objectives is to study how FDS simulates different fire behavior patterns associated to ventilation that can be encountered in many real fire scenarios. Being able to predict or reconstruct accidental fire behavior may be of great value both in firefighting training and education, as well as in forensic studies of arson fires.

The second group of objectives is to analyze how different input variables attributed to user decisions can impact the desired output for which FDS is employed. Fire engineering is a unique field within engineering, as most of the designs and equipment installed will never be tested under accidental fires. Therefore variability in fire simulations may lead to ineffective solutions, putting people's safety at risk.

3. NUMERICAL FIRE MODELING

Simulation of processes is a very powerful tool in many engineering fields due to its time and cost efficiency. In the case of fire dynamics, the output reliability is crucial due to the severe consequences that might result from an erroneous design. Simultaneously, it is well known that fire behavior involves several complex chemical and physical phenomena occurring at the same time: fluid motion of reacting flows, every mode of heat transfer, and phase change, to mention a few.

The modeling of the fire phenomena can be classified in two groups. The first group, which is not considered in this work, consists of probabilistic models, which base their calculations on a series of states transitioning from one to the other, relying on mathematical probabilities rather than in physical and chemical principles that govern fire dynamics. The other group is the deterministic models, in which the various phenomena involved in fires are represented by mathematical equations based on the physical and chemical processes that describe fire. Aside from hand-calculations, deterministic models can be separated in two categories, zone models and CFD models.

Zone models

In fire engineering, zone models typically refer to a modeling technique that divides the space into control volumes, usually organized in two zones: a hot zone and a cold zone. For each control volume, equations for mass and energy transfer are solved numerically. Additionally, for the momentum, information about pressure and velocity at the boundaries is required. This type of model assumes that the hot or upper layer contains all the combustion products which are well mixed and at the same temperature. On the other side, the cold or lower layer is filled with ambient air.

Zone modeling has been widely used and has some applications in fire engineering, but it is imprecise when predicting compartment fires where geometry is not regular, or fires controlled by ventilation.

CFD models

The rapid evolution on computing power and the development of the field of computational fluid dynamics, have led to the use of CFD models, also known as field models, to analyze fire behavior in both research and engineering applications. CFD modeling takes a step further compared to zone models by dividing the room into a large number of tiny cells where changes in each cell are calculated by solving the fundamental equations of fluid dynamics, including the conservation laws for momentum, mass and heat transfer. For every cell, physical conditions are the result of the condition of the adjacent cells. (11)

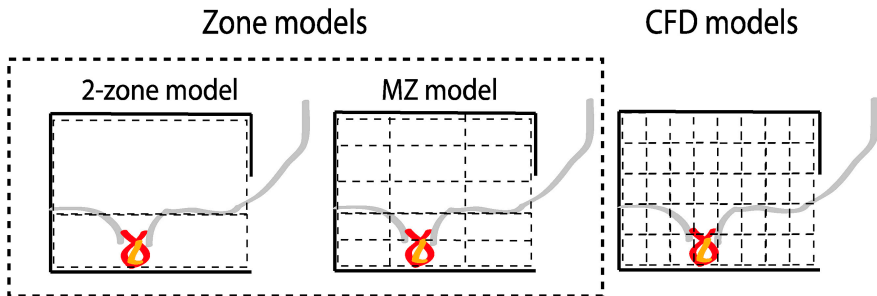


Figure 2.1. Comparison between Zone and CFD models for fire engineering

(Source: Nils Johansson, Evaluation of a zone model for fire safety engineering in large spaces. Fire Safety Journal)

3.1. FIRE DYNAMICS SIMULATOR

The software FDS, developed by NIST, falls into the category of field or CDF modeling. The software solves the fundamental conservation equations of mass and species, momentum and energy transport.

It's worth noting that FDS has been extensively validated through multiple experiments where the model user is provided with extensive and complete information about the scenario, material properties and fire data.

3.1.1. Fundamental conservation equations

The software solves a form of the general equations of fluid dynamics, the Navier-Stokes equations, appropriate for low-speed, thermally driven-flows commonly employed in combustion modeling, where the main driving forces are buoyancy forces due to density variation and heat released by chemical reactions. These modifications of the Navier-Stokes equations are known as low Mach number equations.

While a detailed description of the model is not within the scope of this thesis, the basic equations and the approximations used to model fire dynamics will be presented to allow for an appreciation of the model's capabilities.

Below are the equations used in FDS in their basic form. These equations are modified, by adding terms or adjusting some of the variables to make them appropriate for fire phenomena.

Conservation of mass

$$\frac{\partial \rho}{\partial t} + \nabla \cdot \rho \mathbf{u} = 0 \quad \text{Eq. 3.1}$$

Conservation of momentum

$$\frac{\partial}{\partial t}(\rho \mathbf{u}) + \nabla \cdot \rho \mathbf{u} \mathbf{u} + \nabla p = \rho \mathbf{g} + \mathbf{f}_b + \nabla \cdot \boldsymbol{\tau}_{ij} \quad \text{Eq. 3.2}$$

Conservation of energy

$$\frac{\partial}{\partial t}(\rho h) + \nabla \cdot \rho h \mathbf{u} = \frac{Dp}{Dt} + \dot{q}''' - \dot{q}_b''' - \nabla \cdot \dot{q}''' + \varepsilon \quad \text{Eq. 3.3}$$

3.1.2. The low Mach-number approach

The low Mach number equations usually are used with velocities where the Mach number is less than 0.3; however, FDS validation studies only cover gas velocities with Mach number up

to 0.1. For each cell, temperature, flux velocity and other properties are assumed to be uniform spatially, not with respect to time, and the low Mach number equations are solved using the finite differences method.

For thermally driven flows, it is assumed that pressure changes occurring in the system are not directly responsible for density variations. This approach takes advantage of the difference of scales between the speed of the burning fluid and the acoustic wave propagation in the fluid. Low Mach number equations filter out the wave propagation within the fluid while preserving large temperature and density variation. (10)

The model accounts for pressure variations decomposing the pressure, p , as the sum of two terms: a term for the background pressure, \bar{p} , and a term for the pressure variation due to perturbations, \tilde{p} (5).

$$p = \bar{p} + \tilde{p} \quad \text{Eq. 3.4}$$

The term relative to the background pressure involves time and height variation of the ambient pressure and accounts for atmosphere stratification, thus $\bar{p}(z, t)$. The perturbation pressure term, \tilde{p} , is much smaller but is what really defines the flow field and is related to different forces acting on the fluid such as air or heat introduced into the compartment, hence $\tilde{p}(x, y, z, t)$. In most fire compartment fire scenarios occurring in buildings open to the atmosphere, \bar{p} can be considered constant, and is the only pressure taken into account in the equation of state, and since the background pressure will be either known or can be calculated, the unknowns will be reduced by one.

$$\bar{p} = \frac{\rho R T}{W} \quad \text{Eq. 3.5}$$

This simplification of the compressible Navier-Stokes equations leaves out the acoustic waves, directly influencing the scale required for time steps to numerically solve the equations and prevent stability issues. The reason for this lies in the fact that acoustic waves travel at a much higher speed than the fluid. To avoid divergent results, stability dictates that the time step should be small enough to ensure that the parameters do not move more than one cell in a single time step:

$$\Delta t \leq \frac{\Delta x}{u + c} \quad \text{Eq. 3.6}$$

Where u is the velocity of the fluid in the 'x' direction and c is the speed of sound in the fluid. As we can see in the previous equation for Δt , in order to consider the effect of sound waves, the time step necessary would require a computational power which is not available for most applications.

3.1.3. Turbulence model

Turbulence is probably the most difficult phenomenon to model in fluid dynamics and has a major impact on many quantities of engineering interest, such as velocity, drag force, contaminant concentrations or flow mixing.

While turbulence doesn't have a unique established definition, turbulent flows present some features that are generally accepted: they appear in three-dimensional flows, exist in a multi-scale manner, are unsteady by nature and induce mixing. Turbulence is caused by an excess of kinetic energy that cannot be dissipated by viscosity forces, unlike what would happen in laminar flows. This excess kinetic energy results in vorticity effects that propagate through the flow. These vorticities can be thought of as eddies of different sizes that dissipate kinetic energy, transforming it into heat.

Turbulence mathematical approach can be classified in three main families of models: Direct Numerical Simulation (DNS), Large-Eddy Simulation (LES) and Reynolds-Averaged Navier Stokes Equations (RANS). (6)

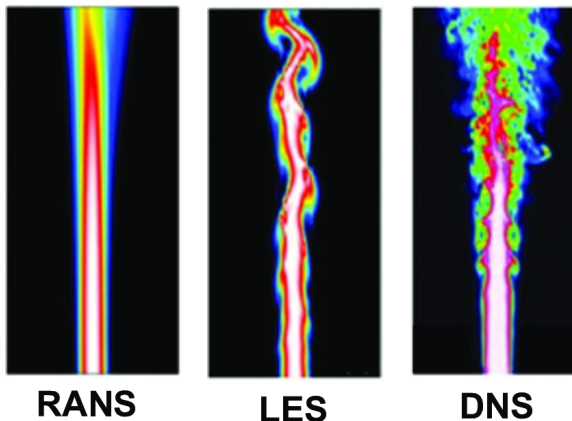


Figure 2.2. Difference between RANS, LES and DNS models for turbulence

(Image from: Larabi, Hakim. (2019). Vers la modélisation multi-composants des flammes de spray.)

The default model used in FDS is the LES model, although the software offers the option to use DNS models and two simplified versions of LES models that can be thought of as hybrid LES-RANS models. In order to understand the limitations of the simulations, the three main strategies for modelling turbulence will be briefly discussed. For clarity, the more accurate method, DNS, will be discussed first since is the less mathematically complex.

3.1.3.1. Direct Numerical Simulation

DNS is the most accurate solution for the Navier-Stokes equations as it resolves all the scales of the turbulence without the necessity of modeling. This is achieved by the use of very small grid sizes and time discretization, allowing for the capture of the effects of all the eddies in the velocity field. In turbulent flows, eddies exist at much different size scales. Kolmogorov introduced the concept of the separation of scales for eddies, which postulates that bigger eddies carry energy that is transferred to the flow and generate more eddies, while smaller eddies dissipate their energy through viscous effects into thermal energy. DNS is able to resolve both scales.

While DNS offers the most accurate solution possible, the computational cost is extremely high, particularly for complex systems at high Reynolds numbers. In fact, computational demands of DNS may exceed the capacity of the available supercomputers. For this reason, DNS is used mainly in a few research fields.

3.1.3.2. Large-Eddy Simulation model

FDS primary model is the large-eddy simulation. The main difference with DNS is that the LES approach, only the larger eddies are solved, while the dissipation effects of the smallest eddies are approximated using what is called the subgrid-scale modelling (SGS).

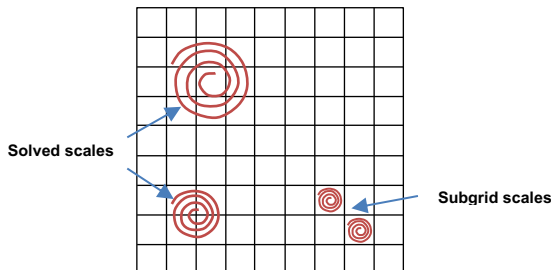


Figure 2.3. Representation of the solved scales of eddies compared to subgrid scale models

In LES simulation, the grid size must be chosen evaluating the compromise between accuracy and simulation time. It is generally accepted that a good LES simulation is one that solves for 80% to 90% of the turbulent kinetic energy of the flow, while the rest is approximated.

To separate the two scales, a filter function must be applied to the Navier-Stokes equations. This results in a modified version of the equations where velocity fluctuations are smoothed out by the filtering operation, as shown in the figure below.

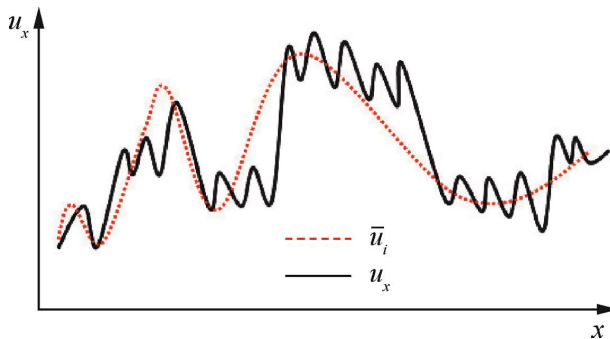


Figure 2.4. Difference between the instantaneous velocity u_x and the filtered velocity \bar{u}_i

(source: Yang Zhiyin. Large-eddy simulation: Past, present and the future. Chinese Journal of Aeronautics - ISSN 1000-9361)

The velocity field can then be separated in to two terms: one for the filtered velocity field, which is resolved, and another term for the velocity fluctuations, that will be modeled.

$$u(x, t) = \bar{u}(x, t) + u'(x, t) \quad \text{Eq. 3.7}$$

By substituting these two terms into the Navier-Stokes and continuity equations, it is possible to group all the terms that account for the unfiltered part of the velocity field and approximate their value using a turbulence model. In the case of FDS, this is Smagorinsky model, which postulates that smaller eddies have a similar effect to viscosity and approximates the energy dissipation by defining a new term dependent on this turbulent viscosity.

Most parameters for the LES model are fixed, but FDS users can adjust specific variables that define the model, such as the filter width or the Smagorinsky constant. Users can also choose to use two simplified versions of the LES model, which involve either simplifying the

SGS model or to model a larger range of eddy scales. These simplifications can be used in order to reduce computational demands while resolving some of the effects of viscosity.

3.1.3.3. Reynolds-Averaged Navier-Stokes model

For many years, the most extensively used model for treating turbulent flows has been the RANS equations. These equations decompose the velocity field into a mean, time averaged velocity in every point in space, plus a fluctuating component that is a function of space and time.

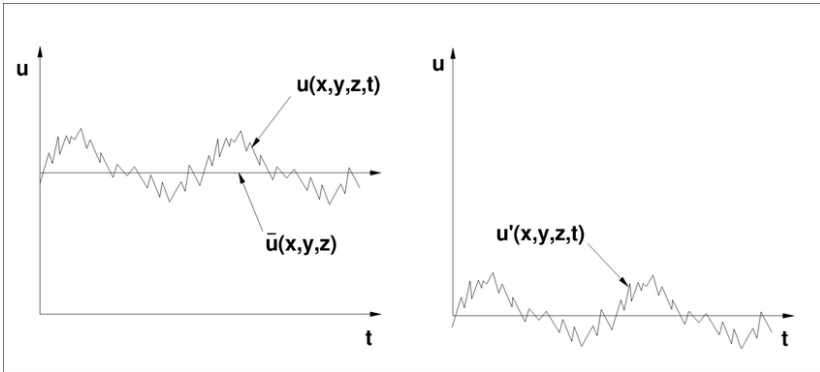


Figure 2.5. representation of the reynolds decomposition of the velocity fileld into the time averaged velocity \bar{u} and the filtered velocity u'

(Source: Make, Michel. (2014). Predicting scale effects on floating offshore wind turbines.)

The 'x' component of the velocity field could, then, be represented as:

$$u(x, t) = \bar{u}(x) + u'(x, t) \quad \text{Eq. 3.8}$$

The RANS equations are obtained plugging this new definition of the velocity field into the Navier-Stokes equations and averaging them over time to obtain a simplified version of the equations which are dependent on the mean flow velocity.

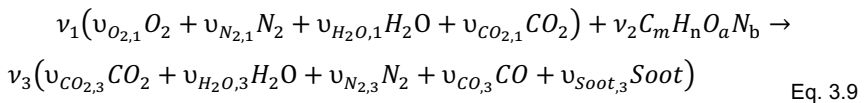
A new term is included that corresponds to the shear stress caused by the fluctuations, known as the Reynolds stresses. In order to eliminate the velocity fluctuations from the equations and have an expression that is solely dependent on the mean flow velocity field, the Reynolds stresses are modeled in a similar way than in LES models, but relative to the mean flow velocity.

The RANS models offer a much higher computational efficiency at the expense of not being able to capture flow complexity. Therefore, they may not reflect features of interest in fire simulations such as mixing and fire spreading.

3.1.4. Combustion model

In order to reduce the number of calculations for each cell, FDS uses a rather simplified approach to modeling combustion. This is achieved by reducing the number of fuels to one, and sometimes two, that take the form of a hydrocarbon $C_mH_nO_aN_b$ and by modeling the reaction is considering just three “grouped species”, named lumped species, that are transported together: fuel, air and products.

The FDS general reaction can be written as follows:



In the reaction, the lumped species are expressed in terms of volume fraction ($v_{i,j}$) of their primitive species. For the previous reaction, lumped specie number 1 is air, and is represented as the primitive species O_2 , N_2 , H_2O and CO_2 based on the volume fraction for each species. The same approach is applied to the products. The amount of CO and soot produced in the reaction has to be defined by the user as the ratio of mass of CO or soot to the mass of fuel reacted. Typical values of soot and CO yields for different reactions can be found in fire safety handbooks, such as the SFPE handbook, as well as in some fire safety regulations.

Once the fuel and the reaction parameters are defined, it is necessary to know how much of the fuel is reacting in each cell at every time step. To this end, each cell is modeled as a turbulent batch reactor where the species are mixed to some degree, and thus, mixing needs to

be modeled. In most cases mixing is controlled by turbulence, but diffusion and buoyancy can also control the mixing rate depending on the flow conditions or cell size. For example, for very small cell size such as the cell size that it would be used in DNS simulation, it is assumed that mixing is controlled by diffusion. For larger cell sizes, the sub-grid models for turbulence are responsible for the mixing process. Buoyant acceleration can control the mixing process for very large cell sizes, such as in wildfires.

To determine the degree of mixing in a cell, the following differential equation is used:

$$\frac{d\xi}{dt} = -\frac{\xi}{\tau_{\text{mix}}} \quad \text{Eq. 3.10}$$

Where the variable ξ is defined as the unmixed fraction of the mass in each cell. The default value for the initial unmixed fraction, ξ_0 , is 1 (completely unmixed). The value of τ_{mix} is the characteristic mixing time, a dynamic parameter that is calculated at every time step. It depends on the process that controls the mixing and is directly related to the cell size and the flow conditions.

Once $\xi(t)$ is determined, which represents how much of the mass of the cell is unmixed, the composition of the mixed zone must be calculated in order to allow the reaction to occur, as only the mixed fraction of the cell will react. Assuming that the mass within a cell remains constant during a time step, it can be represented as the density times the cell volume, $\rho \cdot V_c$. This mass can also be described as the sum of the unmixed and mixed masses, $U(t)$ and $M(t)$. If these masses are expressed in terms of the unmixed fraction, $\xi(t)$, then the following equations can be derived:

$$\begin{aligned} U(t) &= \xi(t) \cdot \rho \cdot V_c \\ M(t) &= [1 - \xi(t)] \cdot \rho \cdot V_c \end{aligned} \quad \text{Eq. 3.11}$$

In order to determine the composition of the mixed zone, $M(t)$ is expressed in terms of the mass fraction of each species. For the species α :

$$m_\alpha(t) = Y_\alpha(t) \cdot M(t) \quad \text{Eq. 3.12}$$

Taking the derivative with respect to time, on both sides:

$$\frac{dm_{\alpha}(t)}{dt} = M(t) \frac{dY_{\alpha}(t)}{dt} + Y_{\alpha}(t) \frac{dM(t)}{dt} \quad \text{Eq. 3.13}$$

Since FDS assumes that there is no change in mass within the cell during a time step, we can derive the following:

$$\rho \cdot Vc = M(t) + U(t) \quad \text{Eq. 3.14}$$

$$0 = \frac{dM}{dt} + \frac{dU}{dt} \longrightarrow \frac{dM}{dt} = - \frac{dU}{dt}$$

Considering that the composition in the unmixed zone remains constant during a time step and writing the unmixed and mixed masses in terms of the unmixed fraction, an equation can be derived to express the rate of change of the species α in a form that account for both the mixing model and the kinetics.

$$\frac{dm_{\alpha}}{dt} = \rho Vc \left[\frac{\xi Y_{\alpha}^0}{\tau_{\text{mix}}} + (1 - \xi) \frac{dY_{\alpha}}{dt} \right] \quad \text{Eq. 3.15}$$

In this equation, the second term on the right-hand side represents the kinetics of the system. For most applications, an infinitely fast reaction is assumed for the mixed fraction, following a “mixed is burned” approach, based on the limiting reactant. If the default FDS approach is used, the auto-ignition temperature will be adjusted to zero. For simulations where DNS is used and information about the kinetical parameters are available, FDS offers the option to model an Arrhenius-type reaction.

At the end of each time step, the sum of the product between the rates of production of the species and their respective heats of formation is computed to find the heat release rate (HRR), which is a crucial parameter in fire engineering.

3.1.5. Design fire

FDS can model fire in two ways, both based in the reaction defined by the user.

3.1.5.1. Burner fire

The most straightforward way to design a fire is to define an obstruction, which is a rectilinear shape, and set the properties of its surface as a burner. The combustion reaction, heat release rate per unit area (HRRPUA) and the growth curve are required inputs. FDS uses HRRPUA to calculate the mass flow of gas released by the burner, which is then used in the combustion model.

$$\dot{m}_f'' = \frac{f(t) \dot{q}_{user}''}{\Delta H_c} \quad \text{Eq. 3.16}$$

Where $f(t)$ is the defined time ramp at which the heat is released to its peak, \dot{q}_{user}'' is the HRRPUA and ΔH_c is the heat of combustion of the gas phase. This is the most used manner to design fires in many engineering applications. The values for the input variables can be extracted either from reference handbooks or fire safety regulations.

3.1.5.2. Material defined fire

A more sophisticated fire design can be used where physical and chemical properties of the material need to be defined, such as heat of vaporization, conductivity, emissivity and others. While pyrolysis can be modeled in FDS, there is not much data available for most materials. For liquid fuels, vaporization is modeled combining Raoul's law and the Clausius-Clapeyron equation for vapor pressure equilibrium. FDS does not simulate heat convection within the liquid, rather treats the liquid as a solid and computes conduction heat transfer in one dimension.

3.1.6. Energy equation

Provided that FDS considers pressure as a sum of two terms, a constant term that accounts for the background pressure, \bar{p} , and much smaller term that is related pressure variations, \tilde{p} , the energy equation FDS can be expressed in terms of the sensible enthalpy:

$$\frac{\partial}{\partial t}(\rho h_s) + \nabla \cdot \rho h_s \mathbf{u} = \frac{D\bar{p}}{Dt} + \dot{q}''' - \nabla \cdot \dot{q}'' \quad \text{Eq. 3.17}$$

Where \dot{q}''' is the heat release rate due to combustion and \dot{q}'' accounts for the conductive, diffusive and radiative heat fluxes.

$$\dot{q}'' = -k\nabla T - \sum h_{s,\alpha} \rho D_\alpha \nabla Z_\alpha + \dot{q}_r'' \quad \text{Eq. 3.18}$$

The first term on the right-side accounts for conductive heat transfer, where k is the thermal conductivity, the second term accounts for diffusive heat flux, where D_α is the diffusivity of species α , and \dot{q}_r'' represents the radiative flux.

One of the key components in fire modeling is the treatment of radiation transport as radiation is the most critical component of heat transfer in fires. As fires grow, the smoke layer spreads across the space and heat is transferred by radiation from the smoke layer to all the materials in the room leading to the flashover transition where all the present materials become involved in the fire.

The radiation transport equation in FDS is simplified using the following assumptions:

- Smoke is modeled as a gray gas. This allows considering absorption and emission properties independent of the wavelength. This assumption is based on soot being the main controller of thermal radiation in fire scenarios.
- The scattering term of the radiation transport equation is neglected, except when external droplets are modeled, for example when water sprinklers are included in the model.
- The domain is discretized in finite angles. FDS uses 100 angles as the default mode.

$$\mathbf{s} \cdot \nabla I(r, \mathbf{s}) = -\kappa I(r, \mathbf{s}) + \kappa \frac{\sigma T^4}{\pi} \quad \text{Eq. 3.19}$$

Where the term on the left-hand represents the change in radiative intensity along the direction s , the first term on the right-hand side represents the energy lost due to absorption by the medium and the second term on the right-hand describes the energy emitted by the mixture of gas and soot. (9).

4. CONDUCTED SIMULATIONS

Two sets of simulations have been conducted in order to appreciate the strengths and limitations of FDS.

The first set of simulations have the goal of reproducing a scale prop used in firefighting training to show some characteristic fire behavior that firefighters can encounter in real fire scenarios in apartment buildings. This first set of simulations have the intend to be a sort of validation study for these phenomena. The second set of simulations is to evaluate some parameters of interest, as smoke layer height, CO concentration, and others, if a fire occurred in the chemical engineering laboratory of the University of Barcelona's Faculty of Chemistry.

4.1. SCALE MODEL SIMULATIONS

Firefighters encounter different situations when responding to apartment fires. One of the most important factors, both for safety reasons and in order to choose an appropriate extinction strategy is the ventilation of the fire. In other words, what the flow paths of air and smoke in the scenario are and how situations like opening a door or a window break can affect these flow paths. Besides real scale fires, firefighter training uses smaller models that help illustrate much better this changing behavior of fire depending on ventilation conditions.



Figure 3.1. Image of the Barcelona's Fire Department training scale model

Four typical training situations have been reproduced using Barcelona's Fire Department training prop, which consist of a model representing a two-story building with its stairway and openings. The fuel used to reproduce the fire is bioethanol, commonly used in fireplaces.

The training prop has been modeled using a graphical user interphase (GUI), the software Pyrosim, for which a student license has been obtained. This software is used to create the 3D model and to adjust all the necessary parameters to run the calculations with FDS. The aim is to compare the fire behavior in both the real and simulated props.

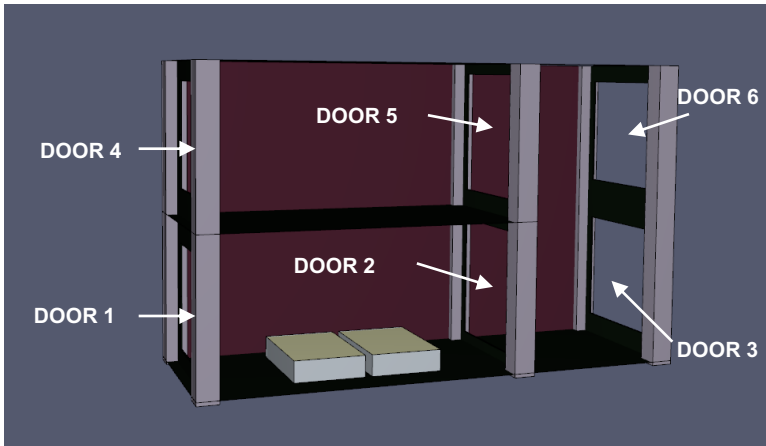


Figure 3.2. Image of the Pyrosim recreation of the scale model

The following phenomena have been reproduced in the scale model, and then simulated in FDS:

4.1.1. Bidirectional fire

In the firefighting community, the term bidirectional fire is used to describe a compartment fire where the inflow of fresh air and the outflow of hot gases, smoke and flames move in opposite directions within the same opening. That is a typical situation when there is only one opening in the room, such as a window, and the door is closed.

These kinds of fires are usually ventilation controlled, which means that oxygen is the limiting factor, this usually results in larger production of unburned gases and soot. Also, this

scenario is more susceptible to backdraft conditions, which is a sudden deflagration of hot unburned gases due to the entrance of fresh air.

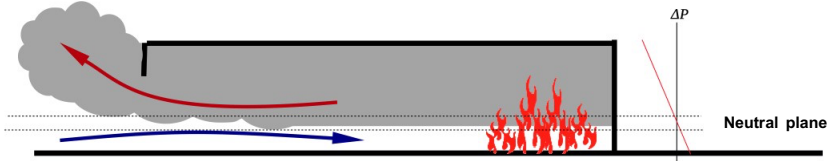


Figure 3.2. Flow paths for a bidirectional fire

(Source: Wikipedia Commons. Author: Art Arnali)

4.1.2. Unidirectional fire

In cases where two openings exist, with a significant pressure difference between them, a single flow will be generated, with fresh air entering through one opening and the fire, hot gases and smoke, exiting through another opening. Such situations can be encountered in apartment buildings when the fire starts on one of the lower floors and the occupants of the burning apartment have evacuated leaving the door open. If a door above the fire to the exterior, such as the rooftop or an upper apartment, is then opened, the flow conditions may change to a bidirectional fire. This is an especially dangerous situation for both occupants and firefighters.

These types of fires are usually fuel controlled, meaning that fuel is the limiting factor, and thus, if there's no suppression, they will burn until there's no more fuel left.

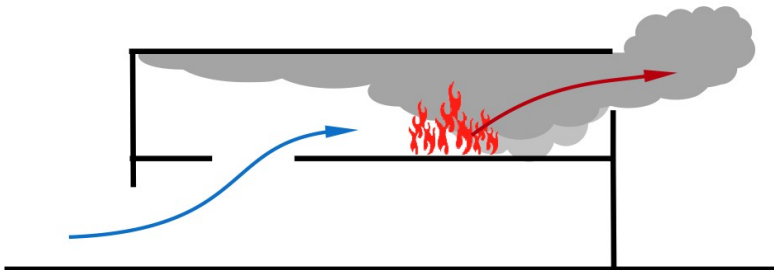


Figure 3.3. Flow paths for a unidirectional fire

(Source: Wikipedia Commons. Author: Art Arnalich)

4.1.3. Pulsating smoke

Pulsating smoke is a phenomenon that may occur in under-ventilated fire when there is not enough oxygen to support combustion. The characteristic feature is the unsteady flow of smoke exiting through the openings in a rhythmic fashion, caused by fluctuations in pressure inside the structure. This is one of the indicators that a sudden opening may lead to a backdraft, which is described in the following subsection.

4.1.4. Backdraft

Backdraft is one of the most feared phenomena among firefighters. There are various definitions for the backdraft; the National Fire Protection Association (NFPA) defines it as a deflagration resulting from the sudden introduction of fresh air into a confined space, such as a room, which contains oxygen-deficient products of an incomplete combustion.

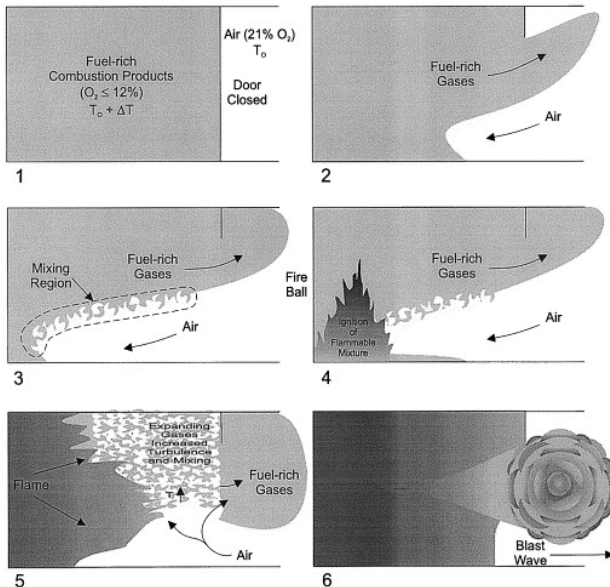


Figure 3.5. Development of a backdraft

(Source: Daniel T. Gottuk, Michelle J. Peatross, John P. Farley, Frederick W. Williams, The development and mitigation of backdraft: a real-scale shipboard study. Fire Safety Journal)

This scenario that can occur when firefighters enter a fire in a compartment that has exhausted most of the air, but the fire remains latent. In the United Kingdom around fifty backdraft situations are reported by firefighters each year. (7)

4.1.5. Simulation Parameters

To simulate the phenomena reproduced in the scale model, the fuel has been modeled in FDS using its physical and chemical properties to allow the material to govern the fire behavior. Since ethanol is one of the few fuels available in the FDS database, for which validation studies have been conducted, the default values have been used. As thermal couples were not available, the main strategy to compare both the real simulation and FDS simulation has been the visual identification of the previous detailed effects. As some of these effects are invisible to the naked eye, a thermal camera used by firefighters has been employed. Additionally, the thermal camera can measure approximate temperatures of the model's surface, and these data can be compared with virtual thermal probes placed in the FDS model.

The simulations have been designed varying two design features: grid size and ignition process.

4.1.5.1. Grid size

The choice of grid size impacts the accuracy of results, especially due to the effects of turbulence sub-grid models, which affect virtually all the interest variables in fire engineering. Two different grid sizes have been employed to compare the effect of the grid size on the simulation outcome. Using very small grid sizes may result in much more accurate results and greater fidelity in the representation of the phenomena, but it requires a significantly higher computing time. Reducing cell size by half results in a calculation time sixteen times higher.

4.1.5.2. Ignition process

The default combustion model in FDS allows reaction to occur if fuel and air are mixed, regardless of the temperature, as piloted ignition is not modeled. Consequently, the default auto-inflammation temperature for all fuels is set to 0 K. This feature of the model is expected to result in an overestimation of the combustion within the domain. FDS guides state that this

model is valid for most well-ventilated fire scenarios. However, since some of the effects modeled in this dissertation occur in under-ventilated conditions, two sets of simulations have been conducted. The first set uses the default auto-ignition FDS process while the second set uses the real value of auto-ignition temperature. In the second set the fire is initiated by modelling hot particles near the ethanol surface to act as an ignition source.

Entry	Simulation	Grid size [m]	Cell number	Turbulence model	Ignition
1	Ventilation 1	0,0125	153.600	LES	Default FDS
2	Ventilation 2	0,025	19.200	LES	Default FDS
3	Ventilation 1	0,0125	153.600	LES	Ignitor particle
4	Ventilation 2	0,025	19.200	LES	Ignitor particle

Table 3.6. Conducted simulations – Scale model simulations

4.2. CHEMICAL ENGINEERING LABORATORY SIMULATIONS

An adapted version of the Chemical Engineering Laboratory at the Universitat de Barcelona has been modeled to analyze how certain input parameters and design decisions can affect the evaluation of variables of interest in fire safety. The laboratory is situated on the sixth floor of the faculty. Although a model of the full building is shown, to reduce computing time, a portion of the sixth floor and the main staircase have been modeled.



Table 3.7. Image of the chemical engineering laboratory modeled in Pyrosim

In order to be able to visualize the smoke distribution and the neutral plane, the ceiling of the laboratory and the back walls have been hidden from the visualization mode.

4.2.1. Simulation Parameters

To evaluate how the output variables change depending on user choices, three input parameters have been modified: grid size, fire location and turbulence model. While grid size and turbulent model have a close relationship, as explained in the previous section, FDS offers the user the choice of simplifying the sub-grid scale model in order to reduce computing time. Fire location, especially in fires near corners within the room, is known to have a significant impact in their due to different air entrapment rates from the fire itself.

The time simulation has been set at 300 s, considering it enough time to evacuate the affected areas of the faculty and for the Barcelona Fire Service to arrive at the incident. The table below shows the different simulations setup.

Entry	Simulation	Grid size [m]	Fire location	Cell number	Turbulence model
1	Room corner Fire 1a	0,4	Corner	144.960	VLES
2	Room corner Fire 1b	0,4	Corner	144.960	LES
3	Room corner Fire 2a	0,2	Corner	1.140.950	VLES
4	Room corner Fire 2b	0,2	Corner	1.140.950	LES
5	Room center fire 1a	0,4	Center	144.960	VLES
6	Room center fire 1b	0,4	Center	144.960	LES
7	Room center fire 2a	0,2	Center	1.140.950	VLES
8	Room center fire 2b	0,2	Center	1.140.950	LES

Table 4. Conducted simulations – Chemical Engineering Laboratory Simulations

The same design fire has been employed in all simulations. The values for the design fire were obtained from the New Zealand building code, since it is one of the few regulations that include guidelines on how to employ simulations in Performance Based Design and has become a global reference code. These parameters define the chemical formula of the fuel to

be employed $\text{CH}_2\text{O}_{0.5}$, which is expressed in the appropriate FDS setup, the yields for soot and CO, and the HRR curve to define based on the building use.

The use of choice was “all buildings”. In order to simulate a plausible fire in the actual chemical engineering laboratory, a fire with a surface of 1,5 m² with a HRR of 660 kW/m² has been modeled.

Table 2.1 Pre-flashover design fire characteristics				
<i>Building use</i>	<i>Fire growth rate (kW)</i>	<i>Species</i>	<i>Radiative fraction</i>	<i>Peak HRR/ HRR/m²</i>
All buildings including storage with a stack height of less than 3.0 m	0.0469 t ²	Y _{soot} = 0.07 kg/kg Y _{CO} = 0.04 kg/kg	0.35	20 MW 500 – 1000 kW/m ² (2) 250 kW/m ² (3)
Carparks (no stacking)	0.0117 t ²	ΔH _c = 20 MJ/kg	0.35	
Capable of storage to a stack height of between 3.0 m and 5.0 m above the floor	0.188 t ²	Y _{CO₂} = 1.5 kg/kg ⁽¹⁾ Y _{H₂O} = 0.82 kg/kg ⁽¹⁾	0.35	50 MW
Capable of storage to a stack height of more than 5.0 m above the floor and car parks with stacking systems	0.00068 t ³ H		0.35	1000–2500 kW/m ² (2) 250 kW/m ² (3)
<p>NOTE: t = time in seconds H = height to which storage is capable of in metres Y = yield kg/kg ΔH_c = heat of combustion (1) As an alternative to CO₂ + H₂O yields use generic fuel as CH₂O_{0.5} and calculate yields. (2) In a CFD model the fire is intended to be modelled as a plan area where the size is determined from the peak HRR/m². A range is provided for HRR/m² to accommodate different HRR and mesh sizes. (3) Use in a zone model.</p>				

Figure 3.8 Values of the design fire of New Zealand building code (C/VM2)

4.2.2. Output Parameters

Different parameters of interest were computed during the simulation to compare the different setups: CO concentration inside the laboratory and at the corridor to the stairway, smoke layer height, and ceiling temperature.

4.2.2.1. CO concentration

The leading cause of death in accidental fires is intoxication due to carbon monoxide. Monitoring time at which lethal concentrations of CO occur in a room is a parameter of interest in fire engineering to ensure the effectiveness of evacuation plans. Concentrations of CO have

been measured inside the lab and in the corridor leading to the staircase at a height of 1,7 m in both cases.

4.2.2.2. *Smoke layer height*

The difference between the room and smoke layer heights defines the neutral plane, which separates clean air from smoke. This parameter directly influences visibility and can impact evacuation routes. Firefighters are also concerned with this parameter, as low visibility can greatly affect rescue and extinguishing operations, as well as the chances of victim survival. Although FDS can compute the smoke layer height, the data is based in temperature measurements and the results do not accurately represent reality. For this reason, visual evaluation has been used at 1 minute and 3 minutes.

4.2.2.3. *Ceiling temperature*

One of the main reasons to use fire simulations in fire design is to analyze the impact of technical solutions that deviate from the prescriptive requirements contained in the fire regulations. A key parameter in these regulations is the fire resistance of the structure, which refers to the amount of time that the building can withstand a fire without structural failure. Fire resistance is typically measured in minutes. Fire simulations can compute the temperature at which structural elements arrive due to the effect of the fire, and then the residual resistance of the element can be evaluated. Thermal pairs have been placed in the ceiling above the fire location to compare how the different simulations can affect the results.

5. RESULTS

5.1. SCALE MODEL SIMULATIONS

The aim of this section is to compare the results obtained in the scale model simulations and compare the effects with the real scale model tests.

The indicators we will focus on to determine the similarities between the real tests and the simulations will be purely visual. Additionally, an approximate temperature will be measured in real-life test and computed in an equivalent location in the simulations. While ignition can be simulated in FDS, is not directly modeled and to recreate it, some manipulations of the scenario are required. While the result may come close to reality, it does not represent it. Nevertheless, ignition has been simulated and will be briefly discussed.

5.1.1. Ventilation behaviour simulations

The first set of simulations have the goal to simulate the changing behavior of the fire due to ventilation. The main interest was to challenge FDS to recreate the changes in the scale model when windows and doors are opened or closed. The simulation is conducted programming the same timing as the one used in the real tests.

The following table describes the sequence of actions of the setup.

Entry	Action	Expected phenomenon	Time [s]
1	Door 1 open	Bidirectional fire	0
2	Door 2 and 3 open	Double bidirectional fire	60
3	Door 3 closed / Door 6 open	Unidirectional fire	80
4	Door 6 closed Door 1 half closed	Pulsating Fire	92

Table 5. Sequence of actions in Ventilation behavior simulations

The simulations were able to reasonably faithfully reproduce the described phenomena. The pictures below compare the observed transitions both in real scale model tests and simulations. For clarity, FDS images include the velocity vector field to allow visualizing the difference in the movement of the flow of fresh air and hot gases in both bidirectional and unidirectional fires.

In both bidirectional fires it is worth noting the deflection effect that air flow has on the lower part flame, leading to the characteristic “mirrored C” shape of the bidirectional fire flames. On the other hand, the unidirectional fire shows a blowtorch type of flame.

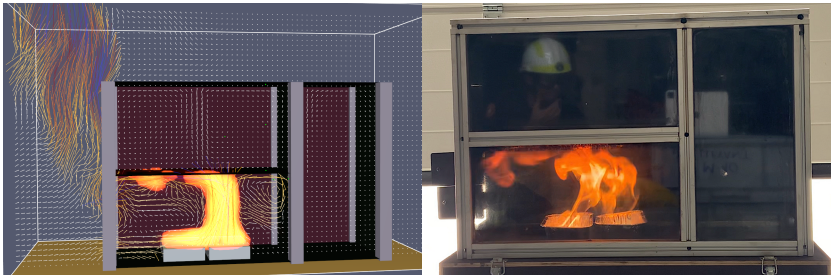


Figure 4.1. Visualization of the bidirectional fire in FDS and real images

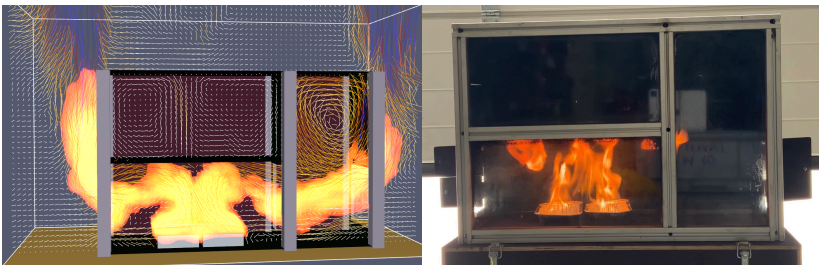


Figure 4.2. Visualization of the double bidirectional fire in FDS and real image



Figure 4.3. Visualization of the unidirectional fire in FDS and real images

The pulsating smoke effect was faithfully reproduced although thermal images in both models had to be used in order to visualize it since ethanol does not produce visible vapors.

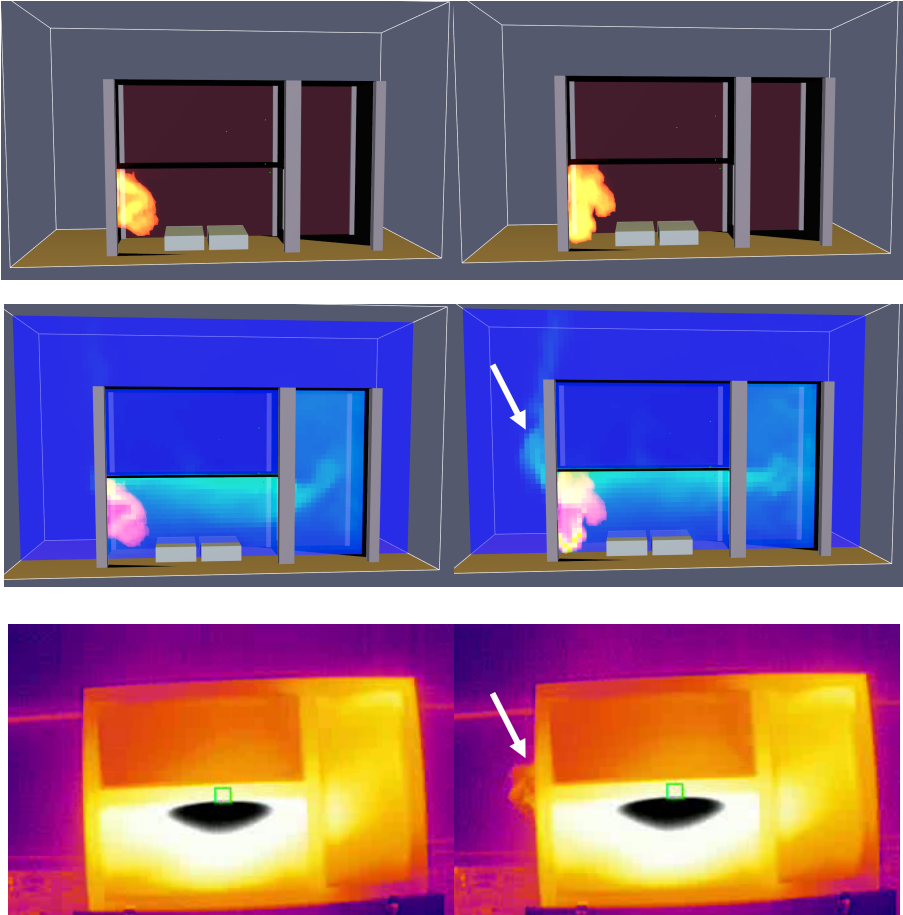


Figure 4.4. Visualization of the pulsating smoke phenomena in FDS and thermal camera images. Column on the right shows the image at one second after the image on the left

The greatest difference observed lie in the overestimation of combustion due to the model used by FDS, which allows the ignition of the cell's fuel solely based on their degree of mixing with the air, regardless of the temperature.

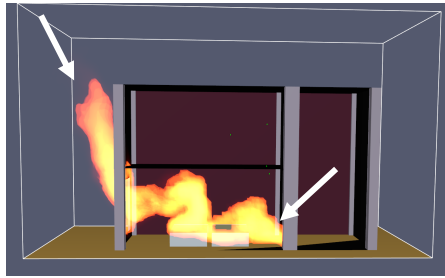


Figure 4.5. Combustion overestimation in FDS due to turbulent mixing controlled ignition

In an attempt to correct false ignition in the domain, another set of simulations was conducted, introducing the autoignition temperature of ethanol, 365 °C, to prevent FDS from allowing combustion at any temperature. Employing the autoignition temperature introduces a new challenge to the simulations: the process of ignition. Since FDS does not allow for setting an ignition temperature, a set of hot particles placed on the surface of the liquid has been modeled in order to heat the nearby vapors above the autoignition temperature and start the fire

The actual autoignition temperature did not provide satisfactory results in simulating the phenomenon, since ignition particles had to remain active for more than half of the simulation time to prevent combustion from self-extinguishing. The cause of this effect could be the difficulty in simulating the heat flux from the flame to the fuel to sustain combustion, as well as the simplification of the chemical kinetics that does not represent intermediate steps, which may be crucial to flame propagation. Additionally, combustion overestimation was still present in these simulations, although not as pronounced.

5.1.2. Backdraft simulation

The final set of simulations aims to represent the backdraft phenomenon. This phenomenon is not always possible to recreate accurately in the real prop, as there are multiple conditions to coincide, such as high temperatures, inadequate ventilation, and a latent fire to ignite the gas mixture when the fresh air enters.

In order to recreate the backdraft in the real model, it is required that the temperature of the prop rises close to 180°C as it was not possible to recreate it at lower temperatures. To save

computational time, the environment temperature in the FDS domain was set to 80°C as the initial temperature. The aim of the simulation was to recreate a possible fire scenario that firefighters could encounter: a ventilation-controlled fire where the entry of firefighters to the apartment lead to the entry of fresh air that mixes with unburned gases and a backdraft happens. The setup was to start with a bidirectional fire, allow it to burn to raise the temperature enough, close the exterior openings to exhaust the oxygen inside the model, and then open the stairway and building doors.

The observed results show significant differences between the simulation and the tests. In the scale model tests, a latent fire was clearly observed when the doors were closed. It was very evident that unburned fuel could ignite anywhere inside the compartment where oxygen was available, even far from the ethanol source. When opening the staircase and the building doors, the scale model demonstrated a delay between the door opening and the ignition, leading to a rapid deflagration originating from the furthest point from the opened door. This showed a deflagration that progressed from the inside to the outside.

During the FDS simulations, the fuel burned almost instantaneously when the exterior door was closed, and oxygen was exhausted. When the staircase and building doors were opened, the unburned gases closer to the door burned instantaneously, showing a deflagration that progressed from the outside to the inside.



Figure 4.6. Sequence of the backdraft simulated in the scale model

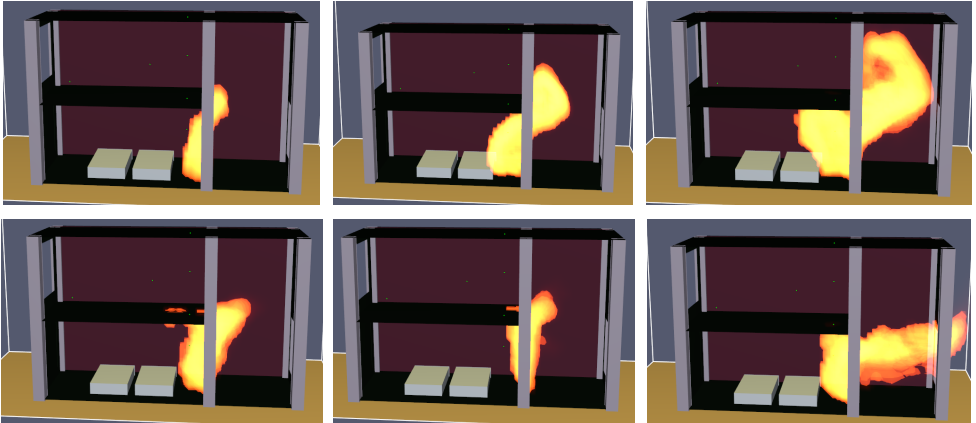


Figure 4.7. Sequence of the backdraft simulated in FDS

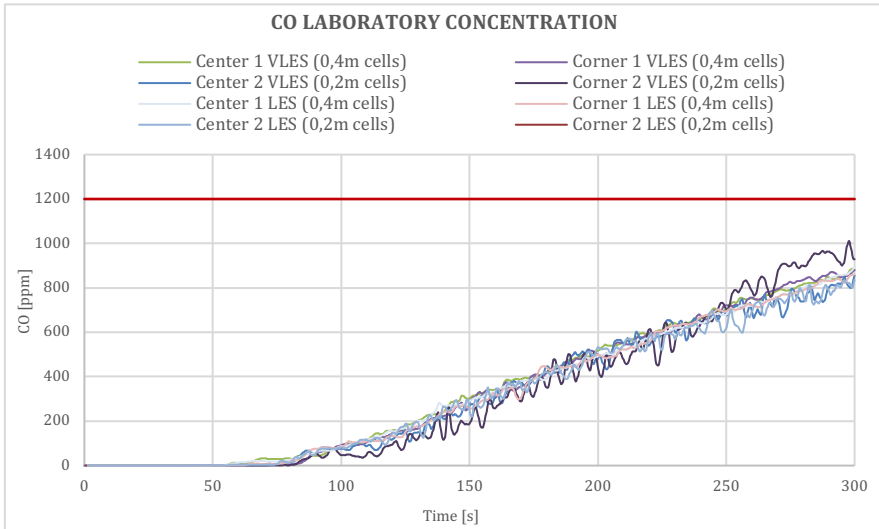
This difference in the observed behavior can be attributed to two reasons. The first reason is the default combustion model used by FDS, where fuel is burned as soon as it is mixed, as the mixing process starts at the near the opened door. The second possible reason could be the door joints in the scale model are not airtight and can sustain a latent fire, unlike in the FDS version of the prop, where door gaps with the structure were not modeled.

5.2. CHEMICAL ENGINEERING LABORATORY SIMULATIONS

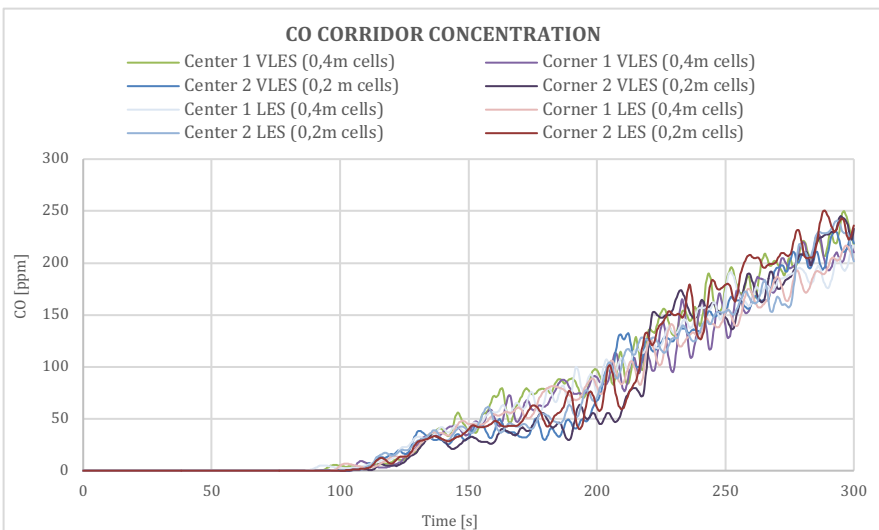
5.2.1. CO concentrations

As a reference concentration for CO toxicity, the IDLH values have been used. IDLH stands for 'Immediately Dangerous to Life or Health' and represent threshold values established by The National Institute for Occupational Safety and Health (NIOSH) of the United States. These values ensure that workers exposed to contaminated environments can escape in the event of protective equipment failure.

CO measurements inside the laboratory and in the corridor leading to the staircase are represented in the graphics below. The horizontal red line represents the IDLH value for CO



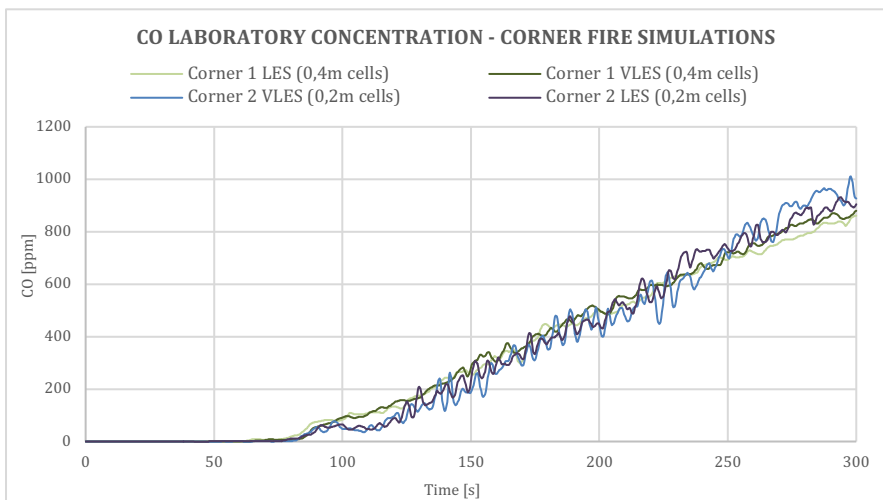
Graphic 1. Evolution of the CO concentration in the Chemical Engineering Laboratory



Graphic 2. Evolution of the CO concentration in the Chemical Engineering Laboratory

The graphics below show that for all simulations CO concentrations would not rise to critical levels for evacuation. Occupants of the laboratory would be expected to leave the room in less than two minutes, a time at which levels near the exit would be under 150 ppm.

All simulations showed similar concentrations of CO, and differences between the values are not considered significant in the context of the safety of the building. Nevertheless, a closer examination of the data reveals how grid size impacts measurement variations. Smaller grid sizes, in both VLES and LES turbulence models, show larger fluctuations in CO concentrations compared to coarser grids, which present smoother results. The reason for this difference may be the sub-grid models used in LES, as larger grid sizes cannot resolve smaller eddies, and thus, results within a cell have to be approximated. The difference in simulation time between 0,4m cells and 0,2m cells was a factor of 16.



Graphic 3. Comparative between different grid sizes using VLES and LES turbulence models

5.2.2. Smoke layer height

No significant variations were found in visual analysis of neutral plane for different simulations. This was an expected result since neither turbulence model nor different grid sizes, from 20cm to 40 cm, should result in large difference of smoke layer height. Different pictures of the corridor at minutes 1 and 3 are shown for different simulations as well as images from the staircase at minute 3.

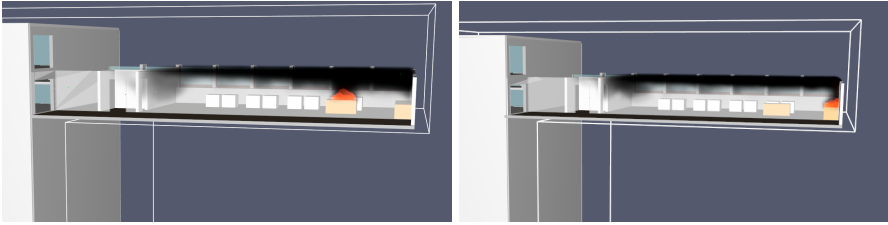


Figure 4.8. Smoke layer in the corridor for center room fire and corner room fire at 1 minute

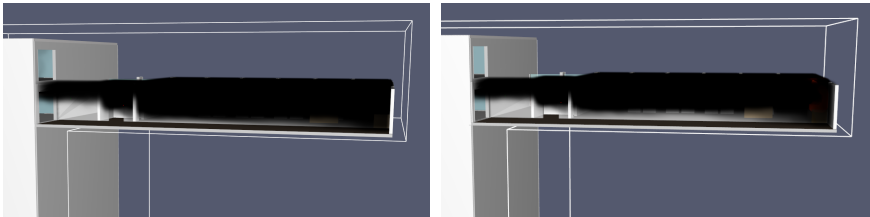


Figure 4.9. Smoke layer in the corridor for center room fire and corner room fire at 3 minutes

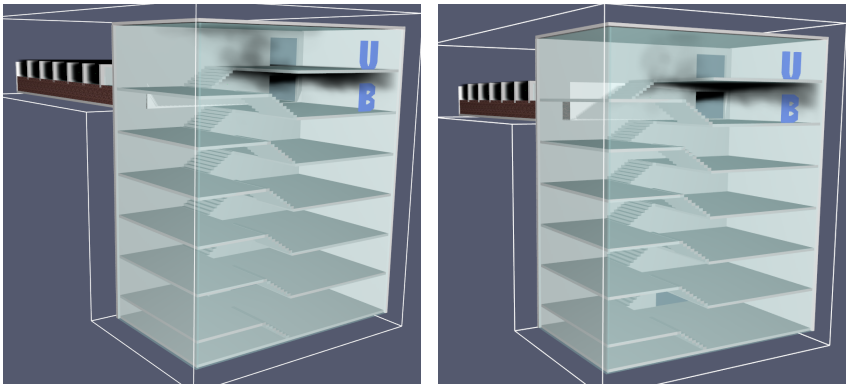
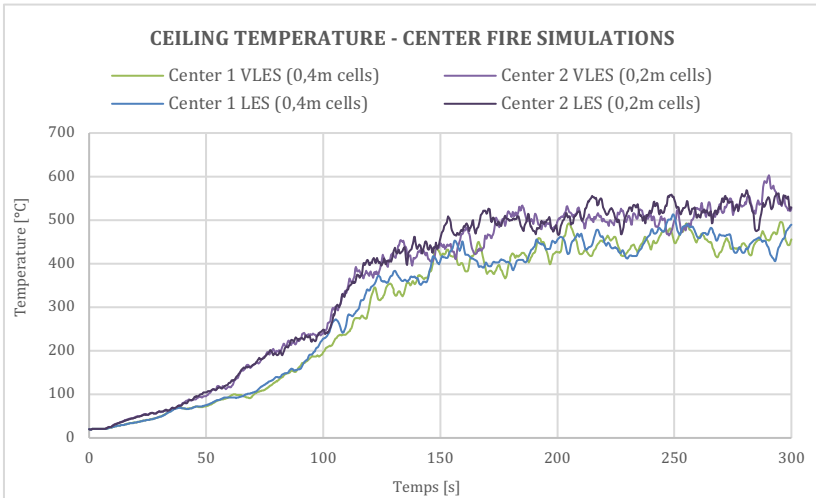


Figure 4.10. Smoke layer in the staircase for center room fire and corner room fire at 3 minutes

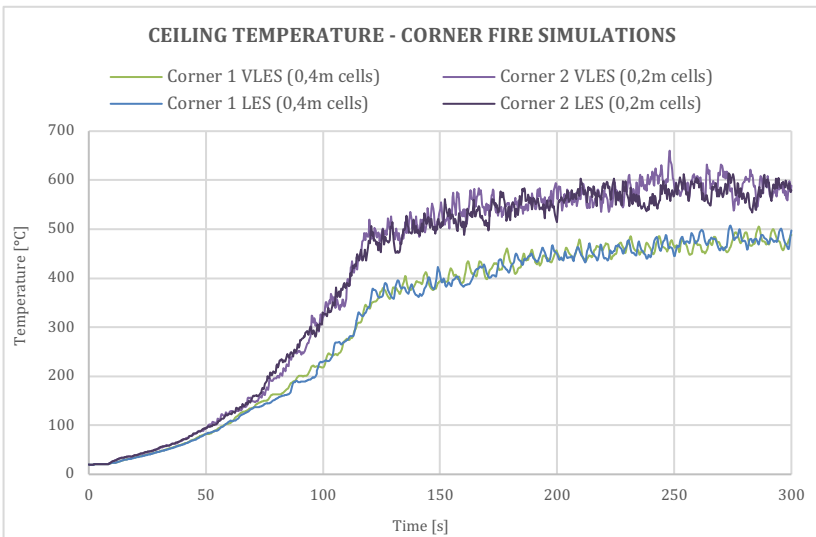
5.2.3. Ceiling temperature

Ceiling temperatures were computed above the two different fire locations, room corner and room center. Two significant differences were observed when analyzing temperature variations. The first difference is attributed to grid size. Reducing grid size by half resulted in a temperature difference of more than 100°C in most cases. The second difference, though less pronounced,

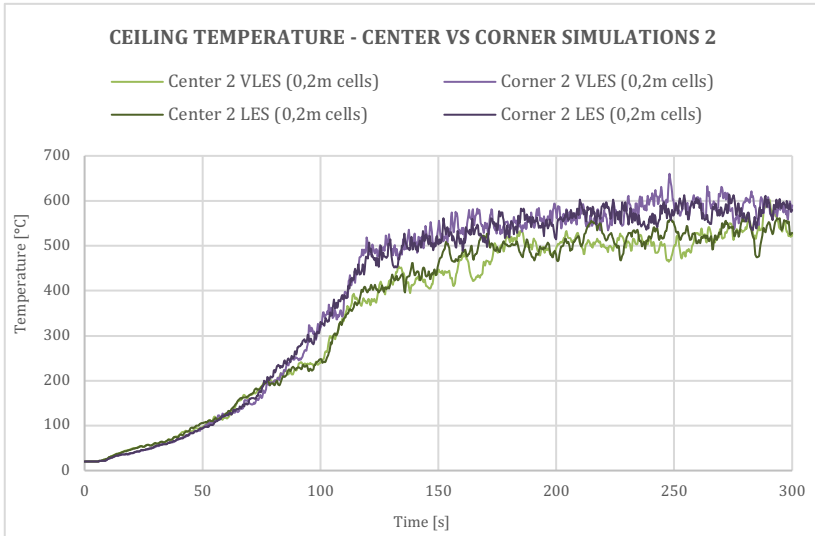
is also a temperature discrepancy when comparing fire locations in smaller grid sizes. Temperatures were nearly 60°C higher in corner fire simulations. Different turbulence models did not show significant variations of temperature. The graphics below illustrate these differences.



Graphic 4. Comparative between temperatures measured in all center fire simulations



Graphic 5. Comparative between temperatures measured in all corner fire simulations



Graphic 5. Comparative between temperatures measured in center fire and corner fire simulations for smaller grid sizes

Differences in temperature can be very relevant in fire engineering when designing building structures, as structural elements are required to maintain sufficient load-bearing capacity for a specified amount of time, depending on building use and height, usually between 30 and 120 minutes. In the data presented, the difference in temperature appears in the range between 500°C and 600°C, the range where steel, one of the main materials used in structures, loses between 30 and 50% of its strength. Fire protection regulations usually base calculations on limiting temperatures in this range of temperatures.

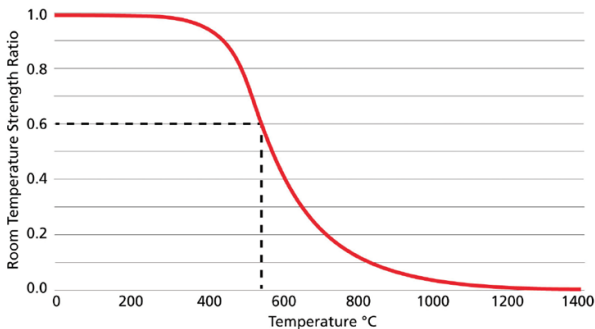
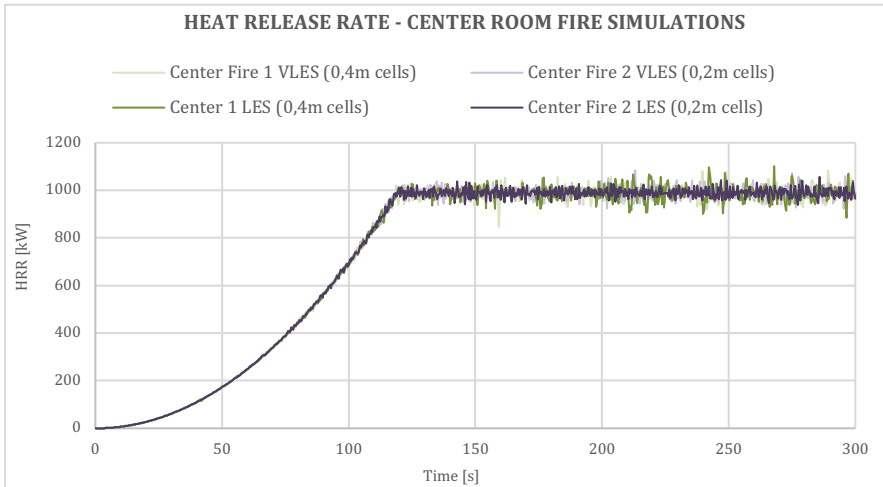


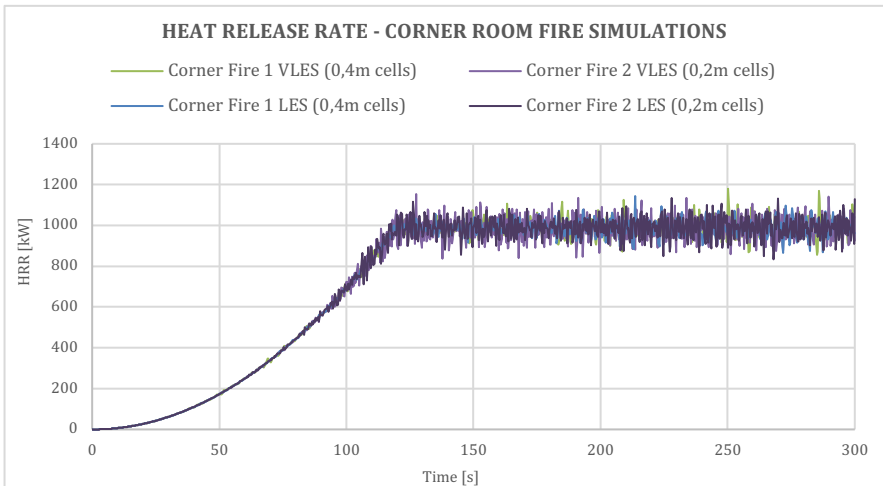
Figure 4.1. Effect of temperature on steel strength

(Source: <https://www.building.co.uk/cpd/cpd-3-2018-steel-and-fire-protection/5091899.article>)

Although the simulations showed different temperature measurements, the data for HRR was very consistent across all simulations. Values for total heat released (THR) were found by integrating the series of HRR over the total simulation time using the trapezoidal integration method.



Graphic 6. Comparative between HRR in center room fire simulations for all grid sizes



Graphic 7. Comparative between HRR in corner room fire simulations for all grid sizes

Entry	Simulation	Turbulence Model	Total Heat Released [kJ]	Mean HRR [kW]
1	Center Fire 1	VLES	218165,76	727,22
2	Center Fire 2	VLES	218119,08	727,06
3	Corner Fire 1	VLES	218118,64	727,06
4	Corner Fire 2	VLES	217384,34	724,61
5	Center Fire 1	LES	218045,43	726,82
6	Center Fire 2	LES	218138,79	727,13
7	Corner Fire 1	LES	218058,91	726,86
8	Corner Fire 2	LES	217655,62	725,52

This result is consistent with the combustion model. While difference in turbulence calculations due to grid size or turbulence model may result in different rates of combustion within each cell, the expected global effect is of an equivalent rate of mixing. In other words, gases and air will mix earlier when the effects of turbulence are more pronounced, but as smoke continues to flow in less turbulent fluxes, equivalent degrees of mixing are expected causing similar levels of burned fuel.

6. CONCLUSIONS

This final section summarizes the conclusions and discusses how the key results may impact various aspects of both fire research and fire engineering.

Firstly, it is crucial to have a comprehensive understanding of both the processes that govern fire phenomena and how simulation software, in this case FDS, models and solves these processes. Simulation software present plausible results, which may mislead inexperienced users. Therefore, it is essential to analyze the output with critical reasoning to avoid the 'black box effect' that the software can cause. While this conclusion may apply to different fields of engineering where simulations are used with the intend substituting experimental data, the use of alternative solutions to regulatory standards in fire engineering may cause harm in general population.

Although FDS has undergone multiple validation studies for known scenarios, many of its applications outside of research involve a significant amount of uncertainty. Validation studies should also be conducted in cases where input parameters are not well established, in order to fully understand the capabilities of FDS. Additionally, sensitivity studies are crucial for determining which input variables specified by the user have the greatest impact on the results.

To prevent unwanted effects to be hidden in simulations, fire regulations that consider performance based design as a possibility for fire protection should include detailed input parameters regarding, not just fuel, reaction and heat release rate, but also other parameters such as location of the fire relative to the room, shape of the fire, an actions that could modify the impact of the fire dynamics, like the breaking of windows caused by thermal stress. Additionally, regulations or reference guides should include the acceptable variation in outputs as grid size diminishes. A good practice would be to start simulations on coarser grids and reduce cell size until no significative different in measurements are registered.

Despite the limitations mentioned above, FDS shows a great potential in fire simulations, particularly in the study of smoke and hot gases dynamics. The research-oriented nature of the

software, as well as the transparency in the model that constructs the software, allows for peer review, providing the necessary context for further development of the software limitations to expand its capabilities.

2. REFERENCES AND NOTES

1. Drysdale, D. *An Introduction to Fire Dynamics*, 3rd Ed; John Wiley & Sons, England
2. Karlsson, B.; Quintiere, James G. *Enclosure Fire Dynamics*, CRC Press, Boca Raton, Florida
3. Quintiere, James G. *Fundamentals of Fire Phenomena*, John Wiley & Sons, England
4. Society of Fire Protection Engineers and National Protection Association. “*The SPFE Handbook of Fire Protection Engineering*”, 2nd Edition, Bethesda, MD
5. Kilian, S. *The FDS pressure equation: Intuitive understanding and solution strategies*, hhpberlin, Ingenieure für Brandschutz GmbH, D-10245 Berlin
6. Labois, M; Lakehal, D.; *Very-Large Eddy Simulation (V-LES) of the flow across a tube bundle*, 2011, Nuclear Engineering and Design, Volume 241
7. Grimwood, P. *Euro Firefighter: Global Firefighting Strategy and Tactics, Command and Control and Firefighter Safety*, Jeremy Mills Publishing, 2008, London, UK
8. Kause Jr., R.F. and Gann, R.G. *Rate of heat release measurements using oxygen consumption. Journal of Fire and Flammability*, (1980)
9. K. McGrattan, S. Hostikka, R. McDermott, J. Floyd, C. Weinschenk, and K. Overholt. *Fire Dynamics Simulator, Technical Reference Guide*. National Institute of Standards and Technology, Gaithersburg, Maryland, USA, and VTT Technical Research Centre of Finland, Espoo, Finland, sixth edition, September 2013.
10. Bell, J.B., Aspden, A.J., Day, M.S, Lijewski, M.J. *Numerical simulation of low Mach number reacting flows*; Center for Computational Science and Engineering, Lawrence Berkeley National Laboratory, Berkeley, California
11. Heng Yeoh, Guan; Kit Yuen, K. *Computational Fluid Dynamics in Fire Engineering*, 2009, Elsevier, Oxford, UK

3. ACRONYMS

CFD: Computational Fluid Dynamics

FDS: Fire Dynamics Simulator

HRR: Heat Release Rate

HRRPUA: Heat Release Rate per Unit Area

THR: Total Heat Released

DNS: Direct Numerical Simulation

LES: Large Eddy Simulations

VLES: Very Large Eddy Simulations

RANS: Reynolds Averaged Navier-Stokes

IDLH: Immediately Dangerous for Life and Health

NIOSH: National Institute for Occupational Safety and Health

NIST: National Institute of Standards and Technology

APPENDICES

4. APPENDIX 1: FDS CODE

6.1. BACKDRAFT SIMULATION

Assaig_2.fds

```

&HEAD CHID='Assaig_2'/
&TIME T_END=80.0/
&DUMP DT_RESTART=300.0, DT_SL3D=0.25/
&MISC SIMULATION_MODE='LES'/

&MESH ID='Mesh01', IJK=80,40,48, XB=0.0,1.0,0.1,0.6,0.0,0.6/

&REAC ID='FDS6 ETHANOL',
  FYI='FDS6 Predefined',
  FUEL='ETHANOL',
  RADIATIVE_FRACTION=0.35/

&RAMP ID='Desactivat_RAMP', T=-0.25, F=1.0/
&RAMP ID='Desactivat_RAMP', T=0.25, F=-1.0/
&RAMP ID='Apagar foc_RAMP', T=4.75, F=1.0/
&RAMP ID='Apagar foc_RAMP', T=5.25, F=-1.0/
&RAMP ID='Control02_RAMP', T=59.75, F=1.0/
&RAMP ID='Control02_RAMP', T=60.25, F=-1.0/
&RAMP ID='Control01_RAMP', T=-0.25, F=1.0/
&RAMP ID='Control01_RAMP', T=0.25, F=-1.0/
&RAMP ID='Control01_RAMP', T=69.75, F=-1.0/
&RAMP ID='Control01_RAMP', T=70.25, F=1.0/
&CTRL ID='Desactivat', FUNCTION_TYPE='CUSTOM', RAMP_ID='Desactivat_RAMP',
LATCH=.FALSE., INPUT_ID='TIME'/
&CTRL ID='Apagar foc', FUNCTION_TYPE='CUSTOM', RAMP_ID='Apagar foc_RAMP',
LATCH=.FALSE., INPUT_ID='TIME'/
&CTRL ID='invert', FUNCTION_TYPE='ALL', LATCH=.FALSE., INITIAL_STATE=.TRUE.,
INPUT_ID='Control02'/
&CTRL ID='Control02', FUNCTION_TYPE='CUSTOM', RAMP_ID='Control02_RAMP',
LATCH=.FALSE., INPUT_ID='TIME'/
&CTRL ID='invert-2', FUNCTION_TYPE='ALL', LATCH=.FALSE., INITIAL_STATE=.TRUE.,
INPUT_ID='Control01'/
&CTRL ID='Control01', FUNCTION_TYPE='CUSTOM', RAMP_ID='Control01_RAMP',
LATCH=.FALSE., INPUT_ID='TIME'/
&CTRL ID='invert-3', FUNCTION_TYPE='ALL', LATCH=.FALSE., INITIAL_STATE=.TRUE.,
INPUT_ID='Desactivat'/
&DEVC ID='THCP Floor_U', QUANTITY='THERMOCOUPLE', XYZ=0.6,0.3,0.215/
&DEVC ID='THCP Cover', QUANTITY='THERMOCOUPLE', XYZ=0.6,0.3,0.43/
&DEVC ID='FLOW', QUANTITY='MASS FLUX', SPATIAL_STATISTIC='SURFACE INTEGRAL',
XB=0.0,1.0,0.325,0.325,0.0,0.6/
&DEVC ID='THCP Centre', QUANTITY='THERMOCOUPLE', XYZ=0.6,0.3,0.33/

```

```
&DEVC ID='Temperatura Etanol Superior', QUANTITY='TEMPERATURE', XYZ=0.28,0.33,0.2475/  
&DEVC ID='TIME', QUANTITY='TIME', XYZ=0.0,0.1,0.0/
```

```
&MATL ID='STEEL',  
FYI='Drysdale, Intro to Fire Dynamics - ATF NIST Multi-Floor Validation',  
SPECIFIC_HEAT=0.46,  
CONDUCTIVITY=45.8,  
DENSITY=7850.0,  
EMISSIVITY=0.95/
```

```
&MATL ID='ALUMINUM',  
SPECIFIC_HEAT=0.9,  
CONDUCTIVITY=200.0,  
DENSITY=2699.0,  
ABSORPTION_COEFFICIENT=7.5,  
EMISSIVITY=0.2/
```

```
&MATL ID='ETHANOL LIQUID',  
FYI='VU Ethanol Pan Fire FDS5 Validation',  
SPECIFIC_HEAT=2.45,  
CONDUCTIVITY=0.17,  
DENSITY=787.0,  
ABSORPTION_COEFFICIENT=1534.3,  
EMISSIVITY=1.0,  
HEAT_OF_REACTION=880.0,  
SPEC_ID(1,1)='ETHANOL',  
NU_SPEC(1,1)=1.0,  
BOILING_TEMPERATURE=76.0/
```

```
&SURF ID='STEEL',  
RGB=18,15,0,  
MATL_ID(1,1)='STEEL',  
MATL_MASS_FRACTION(1,1)=1.0,  
THICKNESS(1)=3.0E-3,  
LAYER_DIVIDE=0.0/
```

```
&SURF ID='ALUMINUM SHEET',  
RGB=175,183,190,  
MATL_ID(1,1)='ALUMINUM',  
MATL_MASS_FRACTION(1,1)=1.0,  
THICKNESS(1)=3.0E-3/
```

```
&SURF ID='FIRE',  
COLOR='RED',  
HRRPUA=500.0,  
TAU_Q=-1.0,  
TMP_FRONT=0.0,  
MASS_FRACTION=1.0,  
SPEC_ID='ETHANOL',  
TAU_MF=1.0/
```

```
&SURF ID='ETHANOL POOL',  
RGB=255,255,204,  
TMP_INNER=40.0,  
MATL_ID(1,1)='ETHANOL LIQUID',  
MATL_MASS_FRACTION(1,1)=1.0,  
THICKNESS(1)=0.02,  
EXTERNAL_FLUX=5/
```

```
&SURF ID='ETHANOL SUPERIOR',
```

```

RGB=146,202,166,
MATL_ID(1,1)=ETHANOL LIQUID',
MATL_MASS_FRACTION(1,1)=1.0,
THICKNESS(1)=0.02/

```

```

&OBST ID='Base', XB=0.2,0.89,0.2,0.45,5.0E-3,5.0E-3, RGB=19,22,16, SURF_ID='STEEL'/
&OBST ID='Floor', XB=0.2,0.67,0.2,0.45,0.215,0.215, RGB=19,22,16, SURF_ID='STEEL'/
&OBST ID='Cover', XB=0.2,0.89,0.2,0.45,0.43,0.43, RGB=19,22,16, SURF_ID='STEEL'/
&OBST ID='Front central profile 1', XB=0.64,0.67,0.2,0.23,0.0,0.43, RGB=145,140,155,
SURF_ID='ALUMINUM SHEET'/
&OBST ID='Front central profile 2', XB=0.64,0.67,0.42,0.45,0.0,0.43, RGB=145,140,155,
SURF_ID='ALUMINUM SHEET'/
&OBST ID='Front right profile 1', XB=0.86,0.89,0.2,0.23,0.0,0.43, RGB=145,140,155,
SURF_ID='ALUMINUM SHEET'/
&OBST ID='Front right profile 2', XB=0.86,0.89,0.42,0.45,0.0,0.43, RGB=145,140,155,
SURF_ID='ALUMINUM SHEET'/
&OBST ID='Front left profile 1', XB=0.2,0.23,0.2,0.23,0.0,0.43, RGB=145,140,155,
SURF_ID='ALUMINUM SHEET'/
&OBST ID='Front left profile 2', XB=0.2,0.23,0.42,0.45,0.0,0.43, RGB=145,140,155,
SURF_ID='ALUMINUM SHEET'/
&OBST ID='Glass 1', XB=0.2,0.89,0.21,0.212,0.0,0.435, COLOR='INVISIBLE'/
&OBST ID='Back wall', XB=0.21,0.88,0.432,0.432,0.0,0.43, RGB=67,33,43, SURF_ID='STEEL'/
&OBST ID='Safata Etanol', XB=0.23,0.33,0.25,0.4,0.2475,0.2475, COLOR='INVISIBLE',
SURF_IDS='ETHANOL SUPERIOR','INERT','INERT', CTRL_ID='Desacivat'/
&OBST ID='Safata Etanol', XB=0.23,0.23,0.25,0.4,0.2175,0.2475, COLOR='INVISIBLE',
SURF_ID='ALUMINUM SHEET', CTRL_ID='Desacivat'/
&OBST ID='Safata Etanol', XB=0.33,0.33,0.25,0.4,0.2175,0.2475, COLOR='INVISIBLE',
SURF_ID='ALUMINUM SHEET', CTRL_ID='Desacivat'/
&OBST ID='Safata Etanol', XB=0.23,0.33,0.25,0.25,0.2175,0.2475, COLOR='INVISIBLE',
SURF_ID='ALUMINUM SHEET', CTRL_ID='Desacivat'/
&OBST ID='Safata Etanol', XB=0.23,0.33,0.4,0.4,0.2175,0.2475, COLOR='INVISIBLE',
SURF_ID='ALUMINUM SHEET', CTRL_ID='Desacivat'/
&OBST ID='Safata Etanol', XB=0.3,0.4,0.25,0.4,0.035,0.035, SURF_IDS='ETHANOL
POOL','INERT','INERT'/
&OBST ID='Safata Etanol', XB=0.3,0.3,0.25,0.4,5.0E-3,0.035, SURF_ID='ALUMINUM SHEET'/
&OBST ID='Safata Etanol', XB=0.4,0.4,0.25,0.4,5.0E-3,0.035, SURF_ID='ALUMINUM SHEET'/
&OBST ID='Safata Etanol', XB=0.3,0.4,0.25,0.25,5.0E-3,0.035, SURF_ID='ALUMINUM SHEET'/
&OBST ID='Safata Etanol', XB=0.3,0.4,0.4,0.4,5.0E-3,0.035, SURF_ID='ALUMINUM SHEET'/
&OBST ID='Obstruction', XB=0.265,0.29,0.28,0.31,5.0E-3,0.03,
SURF_IDS='FIRE','INERT','INERT', CTRL_ID='Apagar foc'/
&OBST ID='Left wall', XB=0.2125,0.2125,0.2625,0.3875,0.025,0.175, RGB=19,22,16,
SURF_ID='STEEL', CTRL_ID='invert'/
&OBST ID='Left wall', XB=0.2125,0.2125,0.2625,0.3875,0.0,0.025, RGB=19,22,16,
SURF_ID='STEEL'/
&OBST ID='Left wall', XB=0.2125,0.2125,0.2125,0.2625,0.0,0.425, RGB=19,22,16,
SURF_ID='STEEL'/
&OBST ID='Left wall', XB=0.2125,0.2125,0.3875,0.4375,0.0,0.425, RGB=19,22,16,
SURF_ID='STEEL'/
&OBST ID='Left wall', XB=0.2125,0.2125,0.2625,0.3875,0.175,0.425, RGB=19,22,16,
SURF_ID='STEEL'/
&OBST ID='Central wall', XB=0.65,0.6625,0.25,0.4,0.025,0.2, RGB=19,22,16, SURF_ID='STEEL',
CTRL_ID='invert-2'/
&OBST ID='Central wall', XB=0.65,0.6625,0.25,0.4,0.2375,0.4125, RGB=19,22,16,
SURF_ID='STEEL', CTRL_ID='invert-3'/
&OBST ID='Central wall', XB=0.65,0.6625,0.25,0.4,0.0,0.025, RGB=19,22,16, SURF_ID='STEEL'/

```

```
&OBST ID='Central wall', XB=0.65,0.6625,0.2125,0.25,0.0,0.425, RGB=19,22,16,
SURF_ID='STEEL'/
&OBST ID='Central wall', XB=0.65,0.6625,0.4,0.4375,0.0,0.425, RGB=19,22,16,
SURF_ID='STEEL'/
&OBST ID='Central wall', XB=0.65,0.6625,0.25,0.4,0.2,0.2375, RGB=19,22,16,
SURF_ID='STEEL'/
&OBST ID='Central wall', XB=0.65,0.6625,0.25,0.4,0.4125,0.425, RGB=19,22,16,
SURF_ID='STEEL'/
&OBST ID='Right wall', XB=0.875,0.875,0.25,0.4,0.25,0.4, RGB=19,22,16, SURF_ID='STEEL',
CTRL_ID='invert-3'/
&OBST ID='Right wall', XB=0.875,0.875,0.25,0.4,0.0375,0.1875, RGB=19,22,16,
SURF_ID='STEEL', CTRL_ID='invert-2'/
&OBST ID='Right wall', XB=0.875,0.875,0.25,0.4,0.0,0.0375, RGB=19,22,16, SURF_ID='STEEL'/
&OBST ID='Right wall', XB=0.875,0.875,0.2125,0.25,0.0,0.425, RGB=19,22,16,
SURF_ID='STEEL'/
&OBST ID='Right wall', XB=0.875,0.875,0.4,0.4375,0.0,0.425, RGB=19,22,16,
SURF_ID='STEEL'/
&OBST ID='Right wall', XB=0.875,0.875,0.25,0.4,0.1875,0.25, RGB=19,22,16,
SURF_ID='STEEL'/
&OBST ID='Right wall', XB=0.875,0.875,0.25,0.4,0.4,0.425, RGB=19,22,16, SURF_ID='STEEL'/

&HOLE ID='Left hole 3', XB=0.2,0.24,0.26,0.39,0.3275,0.4025, COLOR='INVISIBLE'/
&HOLE ID='Left hole 4', XB=0.2,0.24,0.26,0.39,0.2535,0.3285, COLOR='INVISIBLE'/
&HOLE ID='Top hole', XB=0.675,0.8625,0.225,0.425,0.45,0.5, COLOR='INVISIBLE',
CTRL_ID='Desactivat'/

&VENT ID='Mesh Vent: Mesh01 [XMAX]', SURF_ID='OPEN', XB=1.0,1.0,0.1,0.6,0.0,0.6/
&VENT ID='Mesh Vent: Mesh01 [XMIN]', SURF_ID='OPEN', XB=0.0,0.0,0.1,0.6,0.0,0.6/
&VENT ID='Mesh Vent: Mesh01 [YMAX]', SURF_ID='OPEN', XB=0.0,1.0,0.6,0.6,0.0,0.6/
&VENT ID='Mesh Vent: Mesh01 [YMIN]', SURF_ID='OPEN', XB=0.0,1.0,0.1,0.1,0.0,0.6/
&VENT ID='Mesh Vent: Mesh01 [ZMAX]', SURF_ID='OPEN', XB=0.0,1.0,0.1,0.6,0.6,0.6/

&SLCF QUANTITY='TEMPERATURE', ID='Temperature', PBY=0.3/
&SLCF QUANTITY='VELOCITY', VECTOR=.TRUE., ID='Moviment aire', PBY=0.27/
&SLCF QUANTITY='MASS FLUX Z', SPEC_ID='ETHANOL', VECTOR=.TRUE., ID='Evaporació',
PBY=0.3/

&TAIL /
```

6.2. VENTILATION PATTERNS SIMULATIONS

Assaig_Uni_Bi_Pulsant.fds

```

&HEAD CHID='Assaig_Uni_Bi_Pulsant'/
&TIME T_END=140.0/
&DUMP DT_RESTART=300.0, DT_SL3D=0.25/
&MISC TMPA=25.0, SIMULATION_MODE='LES'/

&MESH ID='Mesh01', IJK=80,40,48, XB=0.0,1.0,0.1,0.6,0.0,0.6/

&REAC ID='FDS6 ETHANOL',
  FYI='FDS6 Predefined',
  FUEL='ETHANOL',
  RADIATIVE_FRACTION=0.35/

&RAMP ID='Apagar foc_RAMP', T=9.75, F=1.0/
&RAMP ID='Apagar foc_RAMP', T=10.25, F=-1.0/
&RAMP ID='Desactivat_RAMP', T=-0.25, F=1.0/
&RAMP ID='Desactivat_RAMP', T=0.25, F=-1.0/
&RAMP ID='Control_L1_RAMP', T=-0.25, F=-1.0/
&RAMP ID='Control_L1_RAMP', T=0.25, F=1.0/
&RAMP ID='Control_L1_RAMP', T=92.75, F=1.0/
&RAMP ID='Control_L1_RAMP', T=93.25, F=-1.0/
&RAMP ID='Central Hole 1_RAMP', T=59.75, F=-1.0/
&RAMP ID='Central Hole 1_RAMP', T=60.25, F=1.0/
&RAMP ID='Control01_RAMP', T=-0.25, F=1.0/
&RAMP ID='Control01_RAMP', T=0.25, F=-1.0/
&RAMP ID='Control01_RAMP', T=58.75, F=-1.0/
&RAMP ID='Control01_RAMP', T=59.25, F=1.0/
&RAMP ID='Control01_RAMP', T=77.75, F=1.0/
&RAMP ID='Control01_RAMP', T=78.25, F=-1.0/
&RAMP ID='Control05_RAMP', T=-0.25, F=1.0/
&RAMP ID='Control05_RAMP', T=0.25, F=-1.0/
&RAMP ID='Control05_RAMP', T=80.75, F=-1.0/
&RAMP ID='Control05_RAMP', T=81.25, F=1.0/
&RAMP ID='Control05_RAMP', T=91.75, F=1.0/
&RAMP ID='Control05_RAMP', T=92.25, F=-1.0/
&CTRL ID='Apagar foc', FUNCTION_TYPE='CUSTOM', RAMP_ID='Apagar foc_RAMP',
LATCH=.FALSE., INPUT_ID='TIME'/
&CTRL ID='invert', FUNCTION_TYPE='ALL', LATCH=.FALSE., INITIAL_STATE=.TRUE.,
INPUT_ID='Desactivat'/
&CTRL ID='Desactivat', FUNCTION_TYPE='CUSTOM', RAMP_ID='Desactivat_RAMP',
LATCH=.FALSE., INPUT_ID='TIME'/
&CTRL ID='invert-2', FUNCTION_TYPE='ALL', LATCH=.FALSE., INITIAL_STATE=.TRUE.,
INPUT_ID='Control_L1'/
&CTRL ID='Control_L1', FUNCTION_TYPE='CUSTOM', RAMP_ID='Control_L1_RAMP',
LATCH=.FALSE., INPUT_ID='TIME'/
&CTRL ID='invert-3', FUNCTION_TYPE='ALL', LATCH=.FALSE., INITIAL_STATE=.TRUE.,
INPUT_ID='Central Hole 1'/
&CTRL ID='Central Hole 1', FUNCTION_TYPE='CUSTOM', RAMP_ID='Central Hole 1_RAMP',
LATCH=.FALSE., INPUT_ID='TIME'/
&CTRL ID='invert-4', FUNCTION_TYPE='ALL', LATCH=.FALSE., INITIAL_STATE=.TRUE.,
INPUT_ID='Control01'/
&CTRL ID='Control01', FUNCTION_TYPE='CUSTOM', RAMP_ID='Control01_RAMP',
LATCH=.FALSE., INPUT_ID='TIME'/

```

```
&CTRL ID='invert-5', FUNCTION_TYPE='ALL', LATCH=.FALSE., INITIAL_STATE=.TRUE.,
INPUT_ID='Control05'/
&CTRL ID='Control05', FUNCTION_TYPE='CUSTOM', RAMP_ID='Control05_RAMP',
LATCH=.FALSE., INPUT_ID='TIME'/
&DEVC ID='THCP Floor_U', QUANTITY='THERMOCOUPLE', XYZ=0.6,0.3,0.215/
&DEVC ID='THCP Cover', QUANTITY='THERMOCOUPLE', XYZ=0.6,0.3,0.43/
&DEVC ID='FLOW', QUANTITY='MASS FLUX', SPATIAL_STATISTIC='SURFACE INTEGRAL',
XB=0.0,1.0,0.325,0.325,0.0,0.6/
&DEVC ID='THCP Centre', QUANTITY='THERMOCOUPLE', XYZ=0.6,0.3,0.33/
&DEVC ID='Temperatura Aluminu In', QUANTITY='WALL TEMPERATURE', XYZ=0.64,0.227,0.2,
IOR=-3/
&DEVC ID='Glass Temperature', QUANTITY='WALL TEMPERATURE', XYZ=0.6,0.21,0.2, IOR=-
3/
&DEVC ID='Aluminum Temperature Out', QUANTITY='TEMPERATURE',
XYZ=0.653403,0.2,1.375/
&DEVC ID='TIME', QUANTITY='TIME', XYZ=0.0,0.1,0.0/

&MATL ID='STEEL',
FYI='Drysedale, Intro to Fire Dynamics - ATF NIST Multi-Floor Validation',
SPECIFIC_HEAT=0.46,
CONDUCTIVITY=45.8,
DENSITY=7850.0,
EMISSION=0.95/
&MATL ID='ALUMINUM',
SPECIFIC_HEAT=0.9,
CONDUCTIVITY=200.0,
DENSITY=2699.0,
ABSORPTION_COEFFICIENT=7.5,
EMISSION=0.2/
&MATL ID='ETHANOL LIQUID',
FYI='VU Ethanol Pan Fire FDS5 Validation',
SPECIFIC_HEAT=2.45,
CONDUCTIVITY=0.17,
DENSITY=787.0,
ABSORPTION_COEFFICIENT=1534.3,
EMISSION=1.0,
HEAT_OF_REACTION=880.0,
SPEC_ID(1,1)='ETHANOL',
NU_SPEC(1,1)=1.0,
BOILING_TEMPERATURE=76.0/
&MATL ID='GLASS',
SPECIFIC_HEAT=0.84,
CONDUCTIVITY=0.76,
DENSITY=2700.0,
EMISSION=0.89/

&SURF ID='STEEL',
RGB=18,15,0,
MATL_ID(1,1)='STEEL',
MATL_MASS_FRACTION(1,1)=1.0,
THICKNESS(1)=3.0E-3,
LAYER_DIVIDE=0.0/
&SURF ID='ALUMINUM SHEET',
RGB=175,183,190,
```

```

MATL_ID(1,1)='ALUMINUM',
MATL_MASS_FRACTION(1,1)=1.0,
THICKNESS(1)=3.0E-3/
&SURF ID='FIRE',
COLOR='RED',
HRRPUA=700.0,
TAU_Q=-1.0,
TMP_FRONT=0.0,
MASS_FRACTION=1.0,
SPEC_ID='ETHANOL',
TAU_MF=1.0/
&SURF ID='ETHANOL POOL',
RGB=255,255,204,
TMP_INNER=25.0,
MATL_ID(1,1)='ETHANOL LIQUID',
MATL_MASS_FRACTION(1,1)=1.0,
THICKNESS(1)=0.02/
&SURF ID='GLASS',
RGB=255,255,255,
TRANSPARENCY=0.019608,
MATL_ID(1,1)='GLASS',
MATL_MASS_FRACTION(1,1)=1.0,
THICKNESS(1)=4.0E-3/

&OBST ID='Base', XB=0.2,0.89,0.2,0.45,5.0E-3,5.0E-3, RGB=19,22,16, SURF_ID='STEEL'/
&OBST ID='Floor', XB=0.2,0.67,0.2,0.45,0.215,0.215, RGB=19,22,16, SURF_ID='STEEL'/
&OBST ID='Front central profile 1', XB=0.64,0.67,0.2,0.23,0.0,0.43, RGB=145,140,155,
SURF_ID='ALUMINUM SHEET'/
&OBST ID='Front central profile 2', XB=0.64,0.67,0.42,0.45,0.0,0.43, RGB=145,140,155,
SURF_ID='ALUMINUM SHEET'/
&OBST ID='Front right profile 1', XB=0.86,0.89,0.2,0.23,0.0,0.43, RGB=145,140,155,
SURF_ID='ALUMINUM SHEET'/
&OBST ID='Front right profile 2', XB=0.86,0.89,0.42,0.45,0.0,0.43, RGB=145,140,155,
SURF_ID='ALUMINUM SHEET'/
&OBST ID='Front left profile 1', XB=0.2,0.23,0.2,0.23,0.0,0.43, RGB=145,140,155,
SURF_ID='ALUMINUM SHEET'/
&OBST ID='Front left profile 2', XB=0.2,0.23,0.42,0.45,0.0,0.43, RGB=145,140,155,
SURF_ID='ALUMINUM SHEET'/
&OBST ID='Glass 1', XB=0.2,0.89,0.21,0.21,0.0,0.43, COLOR='INVISIBLE', SURF_ID='GLASS'/
&OBST ID='Back wall', XB=0.21,0.88,0.432,0.432,0.0,0.43, RGB=67,33,43, SURF_ID='STEEL'/
&OBST ID='Safata Etanol', XB=0.34,0.44,0.25,0.4,0.035,0.035, SURF_IDS='ETHANOL
POOL','INERT','INERT'/
&OBST ID='Safata Etanol', XB=0.34,0.34,0.25,0.4,5.0E-3,0.035, SURF_ID='ALUMINUM SHEET'/
&OBST ID='Safata Etanol', XB=0.44,0.44,0.25,0.4,5.0E-3,0.035, SURF_ID='ALUMINUM SHEET'/
&OBST ID='Safata Etanol', XB=0.34,0.44,0.25,0.25,5.0E-3,0.035, SURF_ID='ALUMINUM
SHEET'/
&OBST ID='Safata Etanol', XB=0.34,0.44,0.4,0.4,5.0E-3,0.035, SURF_ID='ALUMINUM SHEET'/
&OBST ID='Safata Etanol', XB=0.45,0.55,0.25,0.4,0.035,0.035, SURF_IDS='ETHANOL
POOL','INERT','INERT'/
&OBST ID='Safata Etanol', XB=0.45,0.45,0.25,0.4,5.0E-3,0.035, SURF_ID='ALUMINUM SHEET'/
&OBST ID='Safata Etanol', XB=0.55,0.55,0.25,0.4,5.0E-3,0.035, SURF_ID='ALUMINUM SHEET'/
&OBST ID='Safata Etanol', XB=0.45,0.55,0.25,0.25,5.0E-3,0.035, SURF_ID='ALUMINUM
SHEET'/
&OBST ID='Safata Etanol', XB=0.45,0.55,0.4,0.4,5.0E-3,0.035, SURF_ID='ALUMINUM SHEET'/
&OBST ID='Encenedor', XB=0.4,0.43,0.3,0.33,0.055,0.08, SURF_IDS='INERT','INERT','FIRE',
CTRL_ID='Apagar foc'/

```

```

&OBST ID='Cover', XB=0.675,0.8625,0.225,0.425,0.425,0.425, RGB=19,22,16,
SURF_ID='STEEL', CTRL_ID='invert/'
&OBST ID='Cover', XB=0.2,0.675,0.225,0.425,0.425,0.425, RGB=19,22,16, SURF_ID='STEEL/'
&OBST ID='Cover', XB=0.2,0.8875,0.2,0.225,0.425,0.425, RGB=19,22,16, SURF_ID='STEEL/'
&OBST ID='Cover', XB=0.2,0.8875,0.425,0.45,0.425,0.425, RGB=19,22,16, SURF_ID='STEEL/'
&OBST ID='Cover', XB=0.8625,0.8875,0.225,0.425,0.425,0.425, RGB=19,22,16,
SURF_ID='STEEL/'
&OBST ID='Left wall', XB=0.2125,0.2125,0.2625,0.3875,0.025,0.1, RGB=19,22,16,
SURF_ID='STEEL', CTRL_ID='invert-2/'
&OBST ID='Left wall', XB=0.2125,0.2125,0.2625,0.3875,0.25,0.4, RGB=19,22,16,
SURF_ID='STEEL', CTRL_ID='invert/'
&OBST ID='Left wall', XB=0.2125,0.2125,0.2625,0.3875,0.0,0.025, RGB=19,22,16,
SURF_ID='STEEL/'
&OBST ID='Left wall', XB=0.2125,0.2125,0.2125,0.2625,0.0,0.425, RGB=19,22,16,
SURF_ID='STEEL/'
&OBST ID='Left wall', XB=0.2125,0.2125,0.3875,0.4375,0.0,0.425, RGB=19,22,16,
SURF_ID='STEEL/'
&OBST ID='Left wall', XB=0.2125,0.2125,0.2625,0.3875,0.1,0.25, RGB=19,22,16,
SURF_ID='STEEL/'
&OBST ID='Left wall', XB=0.2125,0.2125,0.2625,0.3875,0.4,0.425, RGB=19,22,16,
SURF_ID='STEEL/'
&OBST ID='Central wall', XB=0.65,0.6625,0.25,0.4,0.025,0.2, RGB=19,22,16, SURF_ID='STEEL',
CTRL_ID='invert-3/'
&OBST ID='Central wall', XB=0.65,0.6625,0.25,0.4,0.2375,0.4125, RGB=19,22,16,
SURF_ID='STEEL', CTRL_ID='invert/'
&OBST ID='Central wall', XB=0.65,0.6625,0.25,0.4,0.0,0.025, RGB=19,22,16, SURF_ID='STEEL/'
&OBST ID='Central wall', XB=0.65,0.6625,0.2125,0.25,0.0,0.425, RGB=19,22,16,
SURF_ID='STEEL/'
&OBST ID='Central wall', XB=0.65,0.6625,0.4,0.4375,0.0,0.425, RGB=19,22,16,
SURF_ID='STEEL/'
&OBST ID='Central wall', XB=0.65,0.6625,0.25,0.4,0.2,0.2375, RGB=19,22,16,
SURF_ID='STEEL/'
&OBST ID='Central wall', XB=0.65,0.6625,0.25,0.4,0.4125,0.425, RGB=19,22,16,
SURF_ID='STEEL/'
&OBST ID='Right wall', XB=0.875,0.875,0.25,0.4,0.0375,0.1875, RGB=19,22,16,
SURF_ID='STEEL', CTRL_ID='invert-4/'
&OBST ID='Right wall', XB=0.875,0.875,0.25,0.4,0.25,0.4, RGB=19,22,16, SURF_ID='STEEL',
CTRL_ID='invert-5/'
&OBST ID='Right wall', XB=0.875,0.875,0.25,0.4,0.0,0.0375, RGB=19,22,16, SURF_ID='STEEL/'
&OBST ID='Right wall', XB=0.875,0.875,0.2125,0.25,0.0,0.425, RGB=19,22,16,
SURF_ID='STEEL/'
&OBST ID='Right wall', XB=0.875,0.875,0.4,0.4375,0.0,0.425, RGB=19,22,16,
SURF_ID='STEEL/'
&OBST ID='Right wall', XB=0.875,0.875,0.25,0.4,0.1875,0.25, RGB=19,22,16,
SURF_ID='STEEL/'
&OBST ID='Right wall', XB=0.875,0.875,0.25,0.4,0.4,0.425, RGB=19,22,16, SURF_ID='STEEL/'

&HOLE ID='Left hole 2', XB=0.2,0.24,0.26,0.39,0.102,0.177, COLOR='INVISIBLE/'

&VENT ID='Mesh Vent: Mesh01 [XMAX]', SURF_ID='OPEN', XB=1.0,1.0,0.1,0.6,0.0,0.6/
&VENT ID='Mesh Vent: Mesh01 [XMIN]', SURF_ID='OPEN', XB=0.0,0.0,0.1,0.6,0.0,0.6/
&VENT ID='Mesh Vent: Mesh01 [YMAX]', SURF_ID='OPEN', XB=0.0,1.0,0.6,0.6,0.0,0.6/
&VENT ID='Mesh Vent: Mesh01 [YMIN]', SURF_ID='OPEN', XB=0.0,1.0,0.1,0.1,0.0,0.6/
&VENT ID='Mesh Vent: Mesh01 [ZMAX]', SURF_ID='OPEN', XB=0.0,1.0,0.1,0.6,0.6,0.6/

```

```
&SLCF QUANTITY='VELOCITY', VECTOR=.TRUE., ID='Moviment aire', PBY=0.27/  
&SLCF QUANTITY='MASS FLUX Z', SPEC_ID='ETHANOL', VECTOR=.TRUE., ID='Evaporació',  
PBY=0.3/  
&SLCF QUANTITY='TEMPERATURE', CELL_CENTERED=.TRUE., ID='Temperatura interior',  
PBY=0.3/  
&SLCF QUANTITY='TEMPERATURE', CELL_CENTERED=.TRUE., ID='Temperatura vidre',  
PBY=0.21/  
&TAIL /
```

6.3. CHEMICAL ENGINEERING LABORATORY SIMULATIONS

Incendi_cantonada_2_LES.fds

```
&HEAD CHID='Incendi_cantonada_2_LES'/
&TIME T_END=300.0/
&DUMP DT_RESTART=300.0, DT_SL3D=0.25/
&MISC SIMULATION_MODE='LES'/

&MESH ID='Mesh01-04', IJK=95,180,36, XB=4.0,23.0,-7.0,29.0,14.862069,22.0/
&MESH ID='Mesh01-01', IJK=95,70,79, XB=4.0,23.0,-7.0,7.0,-1.0,14.862069/

&SPEC ID='FUEL NZ', FORMULA='CH2O0.5'/

&REAC ID='Reaction NZ',
  FYI='New Zealand Building Code Reaction',
  FUEL='FUEL NZ',
  CO_YIELD=0.04,
  SOOT_YIELD=0.07,
  HEAT_OF_COMBUSTION=2.0E+4,
  RADIATIVE_FRACTION=0.35/

&RAMP ID='Finestra_D_RAMP', T=199.75, F=1.0/
&RAMP ID='Finestra_D_RAMP', T=200.25, F=-1.0/
&RAMP ID='Finestra_RAMP', T=199.75, F=1.0/
&RAMP ID='Finestra_RAMP', T=200.25, F=-1.0/
&RAMP ID='Finestra_E_RAMP', T=199.75, F=1.0/
&RAMP ID='Finestra_E_RAMP', T=200.25, F=-1.0/
&RAMP ID='Finestra_3_RAMP', T=199.75, F=1.0/
&RAMP ID='Finestra_3_RAMP', T=200.25, F=-1.0/
&RAMP ID='Finestra_2_RAMP', T=199.75, F=1.0/
&RAMP ID='Finestra_2_RAMP', T=200.25, F=-1.0/
&RAMP ID='Finestra_1_RAMP', T=199.75, F=1.0/
&RAMP ID='Finestra_1_RAMP', T=200.25, F=-1.0/
&CTRL ID='Finestra_D', FUNCTION_TYPE='CUSTOM', RAMP_ID='Finestra_D_RAMP',
LATCH=.FALSE., INPUT_ID='THCP_Finestra_6'/
&CTRL ID='Finestra', FUNCTION_TYPE='CUSTOM', RAMP_ID='Finestra_RAMP',
LATCH=.FALSE., INPUT_ID='THCP_Finestra_5'/
&CTRL ID='Finestra_E', FUNCTION_TYPE='CUSTOM', RAMP_ID='Finestra_E_RAMP',
LATCH=.FALSE., INPUT_ID='THCP_Finestra_4'/
&CTRL ID='Finestra_3', FUNCTION_TYPE='CUSTOM', RAMP_ID='Finestra_3_RAMP',
LATCH=.FALSE., INPUT_ID='THCP_Finestra_3'/
&CTRL ID='Finestra_2', FUNCTION_TYPE='CUSTOM', RAMP_ID='Finestra_2_RAMP',
LATCH=.FALSE., INPUT_ID='THCP_Finestra_2'/
&CTRL ID='Finestra_1', FUNCTION_TYPE='CUSTOM', RAMP_ID='Finestra_1_RAMP',
LATCH=.FALSE., INPUT_ID='THCP_Finestra_1'/
&DEVC ID='THCP_Finestra_1', QUANTITY='THERMOCOUPLE', XYZ=7.1,11.75,17.4/
&DEVC ID='THCP_Finestra_2', QUANTITY='THERMOCOUPLE', XYZ=7.1,14.75,17.4/
&DEVC ID='THCP_Finestra_3', QUANTITY='THERMOCOUPLE', XYZ=7.1,17.75,17.4/
&DEVC ID='THCP_Finestra_4', QUANTITY='THERMOCOUPLE', XYZ=7.1,20.75,17.4/
&DEVC ID='THCP_Finestra_5', QUANTITY='THERMOCOUPLE', XYZ=7.1,23.25,17.4/
&DEVC ID='THCP_Finestra_6', QUANTITY='THERMOCOUPLE', XYZ=7.1,26.25,17.4/
```

```

&DEVC ID='Detector CO_LAB', QUANTITY='VOLUME FRACTION', SPEC_ID='CARBON
MONOXIDE', XYZ=16.5,11.0,16.55/
&DEVC ID='THCP_Sostre_Foc 1', QUANTITY='THERMOCOUPLE', XYZ=17.0,27.25,17.95/
&DEVC ID='THCP_Sostre_Foc 2', QUANTITY='THERMOCOUPLE', XYZ=14.5,23.75,17.95/
&DEVC ID='Pla neutre LAB->HEIGHT', QUANTITY='LAYER HEIGHT',
XB=10.0,10.0,20.0,20.0,15.0,18.0/
&DEVC ID='Pla neutre LAB->LTEMP', QUANTITY='LOWER TEMPERATURE',
XB=10.0,10.0,20.0,20.0,15.0,18.0/
&DEVC ID='Pla neutre LAB->UTEMP', QUANTITY='UPPER TEMPERATURE',
XB=10.0,10.0,20.0,20.0,15.0,18.0/
&DEVC ID='Pla neutre passadís->HEIGHT', QUANTITY='LAYER HEIGHT',
XB=20.0,20.0,10.0,10.0,15.0,18.0/
&DEVC ID='Pla neutre passadís->LTEMP', QUANTITY='LOWER TEMPERATURE',
XB=20.0,20.0,10.0,10.0,15.0,18.0/
&DEVC ID='Pla neutre passadís->UTEMP', QUANTITY='UPPER TEMPERATURE',
XB=20.0,20.0,10.0,10.0,15.0,18.0/
&DEVC ID='CO Passadís', QUANTITY='VOLUME FRACTION', SPEC_ID='CARBON
MONOXIDE', XYZ=20.0,6.0,16.9/
&DEVC ID='CO Escales', QUANTITY='VOLUME FRACTION', SPEC_ID='CARBON MONOXIDE',
XYZ=13.0,2.2,16.9/

&MATL ID='YELLOW PINE',
  FYI='Quintiere, Fire Behavior - NIST NRC Validation',
  SPECIFIC_HEAT=2.85,
  CONDUCTIVITY=0.14,
  DENSITY=640.0,
  HEAT_OF_COMBUSTION=4500.0,
  N_REACTIONS=1,
  REFERENCE_TEMPERATURE=100.0/
&MATL ID='Vidre',
  SPECIFIC_HEAT=0.84,
  CONDUCTIVITY=0.76,
  DENSITY=2700.0/
&MATL ID='CONCRETE',
  FYI='NBSIR 88-3752 - ATF NIST Multi-Floor Validation',
  SPECIFIC_HEAT=1.04,
  CONDUCTIVITY=1.8,
  DENSITY=2280.0/
&MATL ID='GYPSUM',
  FYI='NBSIR 88-3752 - ATF NIST Multi-Floor Validation',
  SPECIFIC_HEAT=1.09,
  CONDUCTIVITY=0.17,
  DENSITY=930.0/

&SURF ID='Cadires',
  RGB=0,0,102,
  HRRPUA=300.0,
  TAU_Q=-40.0,
  IGNITION_TEMPERATURE=300.0,
  BURN_AWAY=.TRUE.,
  BACKING='INSULATED'/
&SURF ID='Finestra',
  RGB=203,255,255,
  TRANSPARENCY=0.196078,
  BACKING='INSULATED',
  MATL_ID(1,1)='Vidre',

```

```

MATL_MASS_FRACTION(1,1)=1.0,
THICKNESS(1)=0.05/
&SURF ID='Formigó',
COLOR='GRAY 80',
BACKING='INSULATED',
MATL_ID(1,1)='CONCRETE',
MATL_MASS_FRACTION(1,1)=1.0,
THICKNESS(1)=0.2/
&SURF ID='Paret',
COLOR='WHITE',
BACKING='INSULATED',
MATL_ID(1,1)='GYPSUM',
MATL_MASS_FRACTION(1,1)=1.0,
THICKNESS(1)=0.2/
&SURF ID='Façana',
RGB=102,51,0,
TEXTURE_MAP='psm_brick.jpg',
TEXTURE_WIDTH=0.812801,
TEXTURE_HEIGHT=0.812801/
&SURF ID='TERRA',
TEXTURE_MAP='psm_tile.jpg',
TEXTURE_WIDTH=0.21336,
TEXTURE_HEIGHT=0.21336/
&SURF ID='Foc',
COLOR='RED',
HRRPUA=660.0,
TAU_Q=-119.0,
TMP_FRONT=300.0,
MASS_FRACTION=1.0,
SPEC_ID='FUEL NZ',
TAU_MF=1.0/

&OBST ID='Taulell laboratori', XB=7.1,8.463497,10.25,28.0,15.2,16.4, COLOR='GRAY 80'/
&OBST ID='Taulell individual', XB=10.8,12.0,22.5,23.5,15.2,16.1, COLOR='WHITE'/
&OBST ID='Taulell individual', XB=10.8,12.0,23.7,24.7,15.2,16.1, COLOR='WHITE'/
&OBST ID='Taulell individual', XB=10.8,12.0,20.7,21.7,15.2,16.1, COLOR='WHITE'/
&OBST ID='Taulell individual', XB=10.8,12.0,19.5,20.5,15.2,16.1, COLOR='WHITE'/
&OBST ID='Taulell individual', XB=10.8,12.0,14.7,15.7,15.2,16.1, COLOR='WHITE'/
&OBST ID='Taulell individual', XB=10.8,12.0,13.5,14.5,15.2,16.1, COLOR='WHITE'/
&OBST ID='Taulell individual', XB=10.8,12.0,16.5,17.5,15.2,16.1, COLOR='WHITE'/
&OBST ID='Taulell individual', XB=10.8,12.0,17.7,18.7,15.2,16.1, COLOR='WHITE'/
&OBST ID='Taula', XB=14.0,18.0,27.0,28.0,15.2,16.1/
&OBST ID='Taula', XB=14.1,15.1,22.5,24.5,15.2,16.1/
&OBST ID='Paret VI', XB=14.8,15.0,7.3,10.05,15.2,17.95, SURF_ID='Paret'/
&OBST ID='Paret VI', XB=15.0,18.0,7.3,7.5,15.2,17.95, SURF_ID='Paret'/
&OBST ID='Paret escala planta', XB=7.3,22.0,4.0,4.25,15.2,17.95, SURF_ID='Paret'/
&OBST ID='Obstruction', XB=18.0,22.0,28.0,28.2,15.2,17.95, SURF_ID='Paret'/
&OBST ID='Obstruction', XB=7.7,18.0,10.05,10.25,15.2,17.95, SURF_ID='Paret'/
&OBST ID='Paret posterior P6', XB=22.0,22.2,4.2,28.2,15.2,18.15, COLOR='INVISIBLE',
SURF_ID='Paret'/
&OBST ID='Obstruction', XB=6.7,18.0,28.0,28.2,15.2,17.95, SURF_ID='Paret'/
&OBST ID='Obstruction', XB=18.0,18.2,4.25,28.2,15.2,17.95, RGB=255,255,255,
TRANSPARENCY=0.247059, SURF_ID='Paret'/

```

&OBST ID='Finestra', XB=7.0,7.1,25.25,28.0,16.4,17.95, SURF_ID='Finestra',
CTRL_ID='Finestra_D'/
&OBST ID='Finestra', XB=7.0,7.1,22.249479,25.0,16.4,17.95, SURF_ID='Finestra',
CTRL_ID='Finestra'/
&OBST ID='Finestra', XB=7.0,7.1,19.253764,22.0,16.4,17.95, SURF_ID='Finestra',
CTRL_ID='Finestra_E'/
&OBST ID='Finestra', XB=7.0,7.1,16.253764,19.0,16.4,17.95, SURF_ID='Finestra',
CTRL_ID='Finestra_3'/
&OBST ID='Finestra', XB=7.0,7.1,13.253764,16.0,16.4,17.95, SURF_ID='Finestra',
CTRL_ID='Finestra_2'/
&OBST ID='Finestra', XB=7.0,7.1,10.25,13.0,16.4,17.95, SURF_ID='Finestra', CTRL_ID='Finestra
1'/
&OBST ID='Finestra', XB=7.0,7.1,7.25,10.0,16.4,17.95, SURF_ID='Finestra', CTRL_ID='Finestra
1'/
&OBST ID='Finestra', XB=7.0,7.1,4.25,7.0,16.4,17.95, SURF_ID='Finestra', CTRL_ID='Finestra 1'/
&OBST ID='Pilar', XB=6.7,7.7,25.0,25.25,16.4,18.15, SURF_ID='Formigó'/
&OBST ID='Pilar', XB=6.7,7.7,22.0,22.25,16.4,18.15, SURF_ID='Formigó'/
&OBST ID='Pilar', XB=6.7,7.7,19.0,19.25,16.4,18.15, SURF_ID='Formigó'/
&OBST ID='Pilar', XB=6.7,7.7,16.0,16.25,16.4,18.15, SURF_ID='Formigó'/
&OBST ID='Pilar', XB=6.7,7.7,13.0,13.25,16.4,18.15, SURF_ID='Formigó'/
&OBST ID='Pilar', XB=6.7,7.7,10.0,10.25,16.4,18.15, SURF_ID='Formigó'/
&OBST ID='Pilar', XB=6.7,7.7,7.0,7.25,16.4,18.15, SURF_ID='Formigó'/
&OBST ID='Façana Lab', XB=6.7,7.3,4.0,28.0,15.2,16.6, SURF_ID='Façana'/
&OBST ID='Paret posterior P7', XB=22.0,22.2,4.2,28.2,18.15,21.1, COLOR='INVISIBLE',
SURF_ID='Paret'/
&OBST ID='Obstruction', XB=18.0,18.2,4.25,28.2,18.15,20.9, COLOR='INVISIBLE',
SURF_ID='Paret'/
&OBST ID='Obstruction', XB=18.0,22.0,28.0,28.2,18.15,20.9, COLOR='INVISIBLE',
SURF_ID='Paret'/
&OBST ID='Façana Vidre D', XB=4.9,22.0,-6.2,-6.0,0.0,20.85, SURF_ID='Finestra'/
&OBST ID='Façana Vidre MF', XB=4.7,4.9,-6.2,4.0,0.0,20.85, SURF_ID='Finestra'/
&OBST ID='Grao', XB=12.2,12.5,0.5,4.0,15.0,15.2, SURF_ID='Formigó'/
&OBST ID='Grao', XB=11.9,12.2,0.5,4.0,14.8,15.0, SURF_ID='Formigó'/
&OBST ID='Grao', XB=11.6,11.9,0.5,4.0,14.6,14.8, SURF_ID='Formigó'/
&OBST ID='Grao', XB=11.3,11.6,0.5,4.0,14.4,14.6, SURF_ID='Formigó'/
&OBST ID='Grao', XB=11.0,11.3,0.5,4.0,14.2,14.4, SURF_ID='Formigó'/
&OBST ID='Grao', XB=10.7,11.0,0.5,4.0,14.0,14.2, SURF_ID='Formigó'/
&OBST ID='Grao', XB=10.4,10.7,0.5,4.0,13.8,14.0, SURF_ID='Formigó'/
&OBST ID='Grao', XB=10.1,10.4,0.5,4.0,13.6,13.8, SURF_ID='Formigó'/
&OBST ID='Grao', XB=10.1,10.4,-6.0,-2.5,13.6,13.8, SURF_ID='Formigó'/
&OBST ID='Grao', XB=10.4,10.7,-6.0,-2.5,13.4,13.6, SURF_ID='Formigó'/
&OBST ID='Grao', XB=10.7,11.0,-6.0,-2.5,13.2,13.4, SURF_ID='Formigó'/
&OBST ID='Grao', XB=11.0,11.3,-6.0,-2.5,13.0,13.2, SURF_ID='Formigó'/
&OBST ID='Grao', XB=11.3,11.6,-6.0,-2.5,12.8,13.0, SURF_ID='Formigó'/
&OBST ID='Grao', XB=11.6,11.9,-6.0,-2.5,12.6,12.8, SURF_ID='Formigó'/
&OBST ID='Grao', XB=11.9,12.2,-6.0,-2.5,12.4,12.6, SURF_ID='Formigó'/
&OBST ID='Grao', XB=12.2,12.5,-6.0,-2.5,12.2,12.4, SURF_ID='Formigó'/
&OBST ID='Replà Planta', XB=12.5,22.0,-6.0,4.2,15.0,15.2, RGB=223,221,221/
&OBST ID='Replà escala', XB=4.9,10.1,-6.0,4.0,13.6,13.8, RGB=223,221,221/
&OBST ID='Grao', XB=12.2,12.5,0.5,4.0,12.0,12.2, SURF_ID='Formigó'/
&OBST ID='Grao', XB=11.9,12.2,0.5,4.0,11.8,12.0, SURF_ID='Formigó'/
&OBST ID='Grao', XB=11.6,11.9,0.5,4.0,11.6,11.8, SURF_ID='Formigó'/
&OBST ID='Grao', XB=11.3,11.6,0.5,4.0,11.4,11.6, SURF_ID='Formigó'/
&OBST ID='Grao', XB=11.0,11.3,0.5,4.0,11.2,11.4, SURF_ID='Formigó'/
&OBST ID='Grao', XB=10.7,11.0,0.5,4.0,11.0,11.2, SURF_ID='Formigó'/
&OBST ID='Grao', XB=10.4,10.7,0.5,4.0,10.8,11.0, SURF_ID='Formigó'/

&OBST ID='Grao', XB=10.1,10.4,0.5,4.0,10.6,10.8, SURF_ID='Formigó/'
&OBST ID='Grao', XB=10.1,10.4,-6.0,-2.5,10.6,10.8, SURF_ID='Formigó/'
&OBST ID='Grao', XB=10.4,10.7,-6.0,-2.5,10.4,10.6, SURF_ID='Formigó/'
&OBST ID='Grao', XB=10.7,11.0,-6.0,-2.5,10.2,10.4, SURF_ID='Formigó/'
&OBST ID='Grao', XB=11.0,11.3,-6.0,-2.5,10.0,10.2, SURF_ID='Formigó/'
&OBST ID='Grao', XB=11.3,11.6,-6.0,-2.5,9.8,10.0, SURF_ID='Formigó/'
&OBST ID='Grao', XB=11.6,11.9,-6.0,-2.5,9.6,9.8, SURF_ID='Formigó/'
&OBST ID='Grao', XB=11.9,12.2,-6.0,-2.5,9.4,9.6, SURF_ID='Formigó/'
&OBST ID='Grao', XB=12.2,12.5,-6.0,-2.5,9.2,9.4, SURF_ID='Formigó/'
&OBST ID='Replà Planta', XB=12.5,22.0,-6.0,4.0,12.0,12.2, RGB=223,221,221/
&OBST ID='Replà escala', XB=4.9,10.1,-6.0,4.0,10.6,10.8, RGB=223,221,221/
&OBST ID='Grao', XB=12.2,12.5,0.5,4.0,9.0,9.2, SURF_ID='Formigó/'
&OBST ID='Grao', XB=11.9,12.2,0.5,4.0,8.8,9.0, SURF_ID='Formigó/'
&OBST ID='Grao', XB=11.6,11.9,0.5,4.0,8.6,8.8, SURF_ID='Formigó/'
&OBST ID='Grao', XB=11.3,11.6,0.5,4.0,8.4,8.6, SURF_ID='Formigó/'
&OBST ID='Grao', XB=11.0,11.3,0.5,4.0,8.2,8.4, SURF_ID='Formigó/'
&OBST ID='Grao', XB=10.7,11.0,0.5,4.0,8.0,8.2, SURF_ID='Formigó/'
&OBST ID='Grao', XB=10.4,10.7,0.5,4.0,7.8,8.0, SURF_ID='Formigó/'
&OBST ID='Grao', XB=10.1,10.4,0.5,4.0,7.6,7.8, SURF_ID='Formigó/'
&OBST ID='Grao', XB=10.1,10.4,-6.0,-2.5,7.6,7.8, SURF_ID='Formigó/'
&OBST ID='Grao', XB=10.4,10.7,-6.0,-2.5,7.4,7.6, SURF_ID='Formigó/'
&OBST ID='Grao', XB=10.7,11.0,-6.0,-2.5,7.2,7.4, SURF_ID='Formigó/'
&OBST ID='Grao', XB=11.0,11.3,-6.0,-2.5,7.0,7.2, SURF_ID='Formigó/'
&OBST ID='Grao', XB=11.3,11.6,-6.0,-2.5,6.8,7.0, SURF_ID='Formigó/'
&OBST ID='Grao', XB=11.6,11.9,-6.0,-2.5,6.6,6.8, SURF_ID='Formigó/'
&OBST ID='Grao', XB=11.9,12.2,-6.0,-2.5,6.4,6.6, SURF_ID='Formigó/'
&OBST ID='Grao', XB=12.2,12.5,-6.0,-2.5,6.2,6.4, SURF_ID='Formigó/'
&OBST ID='Replà Planta', XB=12.5,22.0,-6.0,4.0,9.0,9.2, RGB=223,221,221/
&OBST ID='Replà escala', XB=4.9,10.1,-6.0,4.0,7.6,7.8, RGB=223,221,221/
&OBST ID='Grao', XB=12.2,12.5,0.5,4.0,6.0,6.2, SURF_ID='Formigó/'
&OBST ID='Grao', XB=11.9,12.2,0.5,4.0,5.8,6.0, SURF_ID='Formigó/'
&OBST ID='Grao', XB=11.6,11.9,0.5,4.0,5.6,5.8, SURF_ID='Formigó/'
&OBST ID='Grao', XB=11.3,11.6,0.5,4.0,5.4,5.6, SURF_ID='Formigó/'
&OBST ID='Grao', XB=11.0,11.3,0.5,4.0,5.2,5.4, SURF_ID='Formigó/'
&OBST ID='Grao', XB=10.7,11.0,0.5,4.0,5.0,5.2, SURF_ID='Formigó/'
&OBST ID='Grao', XB=10.4,10.7,0.5,4.0,4.8,5.0, SURF_ID='Formigó/'
&OBST ID='Grao', XB=10.1,10.4,0.5,4.0,4.6,4.8, SURF_ID='Formigó/'
&OBST ID='Grao', XB=10.1,10.4,-6.0,-2.5,4.6,4.8, SURF_ID='Formigó/'
&OBST ID='Grao', XB=10.4,10.7,-6.0,-2.5,4.4,4.6, SURF_ID='Formigó/'
&OBST ID='Grao', XB=10.7,11.0,-6.0,-2.5,4.2,4.4, SURF_ID='Formigó/'
&OBST ID='Grao', XB=11.0,11.3,-6.0,-2.5,4.0,4.2, SURF_ID='Formigó/'
&OBST ID='Grao', XB=11.3,11.6,-6.0,-2.5,3.8,4.0, SURF_ID='Formigó/'
&OBST ID='Grao', XB=11.6,11.9,-6.0,-2.5,3.6,3.8, SURF_ID='Formigó/'
&OBST ID='Grao', XB=11.9,12.2,-6.0,-2.5,3.4,3.6, SURF_ID='Formigó/'
&OBST ID='Grao', XB=12.2,12.5,-6.0,-2.5,3.2,3.4, SURF_ID='Formigó/'
&OBST ID='Replà Planta', XB=12.5,22.0,-6.0,4.0,6.0,6.2, RGB=223,221,221/
&OBST ID='Replà escala', XB=4.9,10.1,-6.0,4.0,4.6,4.8, RGB=223,221,221/
&OBST ID='Grao', XB=12.2,12.5,0.5,4.0,3.0,3.2, SURF_ID='Formigó/'
&OBST ID='Grao', XB=11.9,12.2,0.5,4.0,2.8,3.0, SURF_ID='Formigó/'
&OBST ID='Grao', XB=11.6,11.9,0.5,4.0,2.6,2.8, SURF_ID='Formigó/'
&OBST ID='Grao', XB=11.3,11.6,0.5,4.0,2.4,2.6, SURF_ID='Formigó/'
&OBST ID='Grao', XB=11.0,11.3,0.5,4.0,2.2,2.4, SURF_ID='Formigó/'
&OBST ID='Grao', XB=10.7,11.0,0.5,4.0,2.0,2.2, SURF_ID='Formigó/'
&OBST ID='Grao', XB=10.4,10.7,0.5,4.0,1.8,2.0, SURF_ID='Formigó/'

&OBST ID='Grao', XB=10.1,10.4,0.5,4.0,1.6,1.8, SURF_ID='Formigó'/
&OBST ID='Grao', XB=10.1,10.4,-6.0,-2.5,1.6,1.8, SURF_ID='Formigó'/
&OBST ID='Grao', XB=10.4,10.7,-6.0,-2.5,1.4,1.6, SURF_ID='Formigó'/
&OBST ID='Grao', XB=10.7,11.0,-6.0,-2.5,1.2,1.4, SURF_ID='Formigó'/
&OBST ID='Grao', XB=11.0,11.3,-6.0,-2.5,1.0,1.2, SURF_ID='Formigó'/
&OBST ID='Grao', XB=11.3,11.6,-6.0,-2.5,0.8,1.0, SURF_ID='Formigó'/
&OBST ID='Grao', XB=11.6,11.9,-6.0,-2.5,0.6,0.8, SURF_ID='Formigó'/
&OBST ID='Grao', XB=11.9,12.2,-6.0,-2.5,0.4,0.6, SURF_ID='Formigó'/
&OBST ID='Grao', XB=12.2,12.5,-6.0,-2.5,0.2,0.4, SURF_ID='Formigó'/
&OBST ID='Replà Planta', XB=12.5,22.0,-6.0,4.0,3.0,3.2, RGB=223,221,221/
&OBST ID='Replà escala', XB=4.9,10.1,-6.0,4.0,1.6,1.8, RGB=223,221,221/
&OBST ID='Replà Planta', XB=4.9,22.0,-6.0,4.0,0.0,0.2, RGB=223,221,221/
&OBST ID='Grao', XB=12.2,12.5,0.5,4.0,17.95,18.15, SURF_ID='Formigó'/
&OBST ID='Grao', XB=11.9,12.2,0.5,4.0,17.75,17.95, SURF_ID='Formigó'/
&OBST ID='Grao', XB=11.6,11.9,0.5,4.0,17.55,17.75, SURF_ID='Formigó'/
&OBST ID='Grao', XB=11.3,11.6,0.5,4.0,17.35,17.55, SURF_ID='Formigó'/
&OBST ID='Grao', XB=11.0,11.3,0.5,4.0,17.15,17.35, SURF_ID='Formigó'/
&OBST ID='Grao', XB=10.7,11.0,0.5,4.0,16.95,17.15, SURF_ID='Formigó'/
&OBST ID='Grao', XB=10.4,10.7,0.5,4.0,16.75,16.95, SURF_ID='Formigó'/
&OBST ID='Grao', XB=10.1,10.4,0.5,4.0,16.55,16.75, SURF_ID='Formigó'/
&OBST ID='Grao', XB=10.1,10.4,-6.0,-2.5,16.55,16.75, SURF_ID='Formigó'/
&OBST ID='Grao', XB=10.4,10.7,-6.0,-2.5,16.35,16.55, SURF_ID='Formigó'/
&OBST ID='Grao', XB=10.7,11.0,-6.0,-2.5,16.15,16.35, SURF_ID='Formigó'/
&OBST ID='Grao', XB=11.0,11.3,-6.0,-2.5,15.95,16.15, SURF_ID='Formigó'/
&OBST ID='Grao', XB=11.3,11.6,-6.0,-2.5,15.75,15.95, SURF_ID='Formigó'/
&OBST ID='Grao', XB=11.6,11.9,-6.0,-2.5,15.55,15.75, SURF_ID='Formigó'/
&OBST ID='Grao', XB=11.9,12.2,-6.0,-2.5,15.35,15.55, SURF_ID='Formigó'/
&OBST ID='Grao', XB=12.2,12.5,-6.0,-2.5,15.15,15.35, SURF_ID='Formigó'/
&OBST ID='Replà Planta', XB=12.5,22.0,-6.0,4.2,17.95,18.15, RGB=223,221,221/
&OBST ID='Replà escala', XB=4.9,10.1,-6.0,4.0,16.55,16.75, RGB=223,221,221/
&OBST ID='Replà Planta', XB=4.7,22.2,-6.2,4.2,20.9,21.1, RGB=223,221,221/
&OBST ID='Paret escala', XB=4.7,22.0,4.0,4.25,0.0,20.9, SURF_ID='Formigó'/
&OBST ID='Paret escala', XB=22.0,22.2,-6.2,4.2,0.0,21.1, SURF_ID='Paret'/
&OBST ID='Lletra B', XB=20.55,20.6125,-4.838897,-4.588897,15.94375,16.38125,
RGB=0,51,255, THICKEN=.TRUE./
&OBST ID='Lletra B', XB=20.675,20.7375,-4.838897,-4.588897,16.56875,17.06875,
RGB=0,51,255, THICKEN=.TRUE./
&OBST ID='Lletra B', XB=20.6125,20.675,-4.838897,-4.588897,16.2,16.45, RGB=0,51,255,
THICKEN=.TRUE./
&OBST ID='Lletra B', XB=20.7375,20.8,-4.838897,-4.588897,16.5375,17.0375, RGB=0,51,255,
THICKEN=.TRUE./
&OBST ID='Lletra B', XB=20.6125,20.675,-4.838897,-4.588897,15.9125,16.1625, RGB=0,51,255,
THICKEN=.TRUE./
&OBST ID='Lletra B', XB=20.675,20.7375,-4.838897,-4.588897,16.23125,16.48125,
RGB=0,51,255, THICKEN=.TRUE./
&OBST ID='Lletra B', XB=20.8,20.8625,-4.838897,-4.588897,16.30625,16.99375, RGB=0,51,255,
THICKEN=.TRUE./
&OBST ID='Lletra B', XB=20.8625,20.925,-4.838897,-4.588897,16.3375,16.9625, RGB=0,51,255,
THICKEN=.TRUE./
&OBST ID='Lletra B', XB=20.675,20.7375,-4.838897,-4.588897,15.88125,16.13125,
RGB=0,51,255, THICKEN=.TRUE./
&OBST ID='Lletra B', XB=20.7375,20.8,-4.838897,-4.588897,16.2625,16.5125, RGB=0,51,255,
THICKEN=.TRUE./
&OBST ID='Lletra B', XB=20.925,20.9875,-4.838897,-4.588897,16.36875,16.93125,
RGB=0,51,255, THICKEN=.TRUE./
&OBST ID='Cadira', XB=17.0,17.5,26.6,27.1,15.6,15.7, COLOR='INVISIBLE', SURF_ID='Cadires'/

&OBST ID='Cadira', XB=17.0,17.5,26.5,26.6,15.6,16.4, COLOR='INVISIBLE', SURF_ID='Cadires/'
&OBST ID='Cadira', XB=17.0,17.5,26.6,27.1,15.6,15.7, COLOR='INVISIBLE', SURF_ID='Cadires/'
&OBST ID='Cadira', XB=17.0,17.5,26.5,26.6,15.6,16.4, COLOR='INVISIBLE', SURF_ID='Cadires/'
&OBST ID='Cadira', XB=16.3,16.8,26.6,27.1,15.6,15.7, COLOR='INVISIBLE', SURF_ID='Cadires/'
&OBST ID='Cadira', XB=16.3,16.8,26.5,26.6,15.6,16.4, COLOR='INVISIBLE', SURF_ID='Cadires/'
&OBST ID='Cadira', XB=16.3,16.8,26.6,27.1,15.6,15.7, COLOR='INVISIBLE', SURF_ID='Cadires/'
&OBST ID='Cadira', XB=16.3,16.8,26.5,26.6,15.6,16.4, COLOR='INVISIBLE', SURF_ID='Cadires/'
&OBST ID='Cadira', XB=8.75,9.25,13.45,13.95,15.6,15.7, COLOR='INVISIBLE',
SURF_ID='Cadires/'
&OBST ID='Cadira', XB=9.25,9.35,13.45,13.95,15.6,16.4, COLOR='INVISIBLE',
SURF_ID='Cadires/'
&OBST ID='Cadira', XB=8.75,9.25,13.45,13.95,15.6,15.7, COLOR='INVISIBLE',
SURF_ID='Cadires/'
&OBST ID='Cadira', XB=9.25,9.35,13.45,13.95,15.6,16.4, COLOR='INVISIBLE',
SURF_ID='Cadires/'
&OBST ID='Cadira', XB=8.75,9.25,14.55,15.05,15.6,15.7, COLOR='INVISIBLE',
SURF_ID='Cadires/'
&OBST ID='Cadira', XB=9.25,9.35,14.55,15.05,15.6,16.4, COLOR='INVISIBLE',
SURF_ID='Cadires/'
&OBST ID='Cadira', XB=8.75,9.25,14.55,15.05,15.6,15.7, COLOR='INVISIBLE',
SURF_ID='Cadires/'
&OBST ID='Cadira', XB=9.25,9.35,14.55,15.05,15.6,16.4, COLOR='INVISIBLE',
SURF_ID='Cadires/'
&OBST ID='Terra planta', XB=6.6,22.2,4.0,28.2,15.060345,15.258621,
SURF_IDS='TERRA','Formigó','Formigó/'
&OBST ID='Sostre planta', XB=6.6,22.2,4.0,28.2,18.034483,18.232759, COLOR='INVISIBLE',
SURF_IDS='TERRA','Formigó','Formigó/'
&OBST ID='Sostre edifici', XB=6.6,22.2,4.0,28.2,20.810345,21.008621, COLOR='INVISIBLE',
SURF_ID='Formigó/'
&OBST ID='Lletra U', XB=19.76875,20.83125,-4.813897,-4.563897,18.1,18.225, RGB=0,51,255,
THICKEN=.TRUE./
&OBST ID='Lletra U', XB=19.675,20.925,-4.813897,-4.563897,18.225,18.35, RGB=0,51,255,
THICKEN=.TRUE./
&OBST ID='Lletra U', XB=19.615,20.115,-4.813897,-4.563897,18.35,18.475, RGB=0,51,255,
THICKEN=.TRUE./
&OBST ID='Lletra U', XB=19.55,20.05,-4.813897,-4.563897,18.475,18.6, RGB=0,51,255,
THICKEN=.TRUE./
&OBST ID='Lletra U', XB=19.51875,20.01875,-4.813897,-4.563897,18.6,20.1, RGB=0,51,255,
THICKEN=.TRUE./
&OBST ID='Lletra U', XB=20.58125,21.08125,-4.813897,-4.563897,18.6,20.1, RGB=0,51,255,
THICKEN=.TRUE./
&OBST ID='Lletra U', XB=20.4875,20.9875,-4.813897,-4.563897,18.35,18.475, RGB=0,51,255,
THICKEN=.TRUE./
&OBST ID='Lletra U', XB=20.55,21.05,-4.813897,-4.563897,18.475,18.6, RGB=0,51,255,
THICKEN=.TRUE./
&OBST ID='Lletra U', XB=19.76875,20.83125,-4.813897,-4.563897,18.1,18.225, RGB=0,51,255,
THICKEN=.TRUE./
&OBST ID='Lletra U', XB=19.675,20.925,-4.813897,-4.563897,18.225,18.35, RGB=0,51,255,
THICKEN=.TRUE./
&OBST ID='Lletra U', XB=19.615,20.115,-4.813897,-4.563897,18.35,18.475, RGB=0,51,255,
THICKEN=.TRUE./
&OBST ID='Lletra U', XB=19.55,20.05,-4.813897,-4.563897,18.475,18.6, RGB=0,51,255,
THICKEN=.TRUE./

&OBST ID='Lletra U', XB=19.51875,20.01875,-4.813897,-4.563897,18.6,20.1, RGB=0,51,255, THICKEN=.TRUE./

&OBST ID='Lletra U', XB=20.58125,21.08125,-4.813897,-4.563897,18.6,20.1, RGB=0,51,255, THICKEN=.TRUE./

&OBST ID='Lletra U', XB=20.4875,20.9875,-4.813897,-4.563897,18.35,18.475, RGB=0,51,255, THICKEN=.TRUE./

&OBST ID='Lletra U', XB=20.55,21.05,-4.813897,-4.563897,18.475,18.6, RGB=0,51,255, THICKEN=.TRUE./

&OBST ID='Lletra B', XB=19.6125,20.1125,-4.838897,-4.588897,15.15,17.15, RGB=0,51,255, THICKEN=.TRUE./

&OBST ID='Lletra B', XB=20.1125,20.55,-4.838897,-4.588897,16.643361,17.15, RGB=0,51,255, THICKEN=.TRUE./

&OBST ID='Lletra B', XB=19.6125,20.1125,-4.838897,-4.588897,15.15,17.15, RGB=0,51,255, THICKEN=.TRUE./

&OBST ID='Lletra B', XB=20.1125,20.55,-4.838897,-4.588897,16.643361,17.15, RGB=0,51,255, THICKEN=.TRUE./

&OBST ID='Lletra B', XB=20.55,20.6125,-4.838897,-4.588897,16.63125,17.13125, RGB=0,51,255, THICKEN=.TRUE./

&OBST ID='Lletra B', XB=20.6125,20.675,-4.838897,-4.588897,16.6,17.1, RGB=0,51,255, THICKEN=.TRUE./

&OBST ID='Lletra B', XB=20.55,20.6125,-4.838897,-4.588897,16.63125,17.13125, RGB=0,51,255, THICKEN=.TRUE./

&OBST ID='Lletra B', XB=20.6125,20.675,-4.838897,-4.588897,16.6,17.1, RGB=0,51,255, THICKEN=.TRUE./

&OBST ID='Lletra B', XB=20.1125,20.551104,-4.838897,-4.588897,15.15052,15.65, RGB=0,51,255, THICKEN=.TRUE./

&OBST ID='Lletra B', XB=20.1125,20.55,-4.838897,-4.588897,15.959492,16.362532, RGB=0,51,255, THICKEN=.TRUE./

&OBST ID='Lletra B', XB=20.55,20.6125,-4.838897,-4.588897,15.16875,15.66875, RGB=0,51,255, THICKEN=.TRUE./

&OBST ID='Lletra B', XB=20.6125,20.675,-4.838897,-4.588897,15.2,15.7, RGB=0,51,255, THICKEN=.TRUE./

&OBST ID='Lletra B', XB=20.8,20.8625,-4.838897,-4.588897,15.29375,16.04375, RGB=0,51,255, THICKEN=.TRUE./

&OBST ID='Lletra B', XB=20.7375,20.8,-4.838897,-4.588897,15.2625,15.7625, RGB=0,51,255, THICKEN=.TRUE./

&OBST ID='Lletra B', XB=20.7375,20.8,-4.838897,-4.588897,15.85,16.1, RGB=0,51,255, THICKEN=.TRUE./

&OBST ID='Lletra B', XB=20.675,20.7375,-4.838897,-4.588897,15.23125,15.73125, RGB=0,51,255, THICKEN=.TRUE./

&OBST ID='Lletra B', XB=20.1125,20.551104,-4.838897,-4.588897,15.15052,15.65, RGB=0,51,255, THICKEN=.TRUE./

&OBST ID='Lletra B', XB=20.1125,20.55,-4.838897,-4.588897,15.959492,16.362532, RGB=0,51,255, THICKEN=.TRUE./

&OBST ID='Lletra B', XB=20.55,20.6125,-4.838897,-4.588897,15.16875,15.66875, RGB=0,51,255, THICKEN=.TRUE./

&OBST ID='Lletra B', XB=20.6125,20.675,-4.838897,-4.588897,15.2,15.7, RGB=0,51,255, THICKEN=.TRUE./

&OBST ID='Lletra B', XB=20.8,20.8625,-4.838897,-4.588897,15.29375,16.04375, RGB=0,51,255, THICKEN=.TRUE./

&OBST ID='Lletra B', XB=20.7375,20.8,-4.838897,-4.588897,15.2625,15.7625, RGB=0,51,255, THICKEN=.TRUE./

&OBST ID='Lletra B', XB=20.7375,20.8,-4.838897,-4.588897,15.85,16.1, RGB=0,51,255, THICKEN=.TRUE./

&OBST ID='Lletra B', XB=20.675,20.7375,-4.838897,-4.588897,15.23125,15.73125, RGB=0,51,255, THICKEN=.TRUE./

&OBST ID='Lletra B', XB=20.8625,20.925,-4.838897,-4.588897,15.325,16.0125, RGB=0,51,255, THICKEN=.TRUE./

&OBST ID='Lletra B', XB=20.925,20.9875,-4.838897,-4.588897,15.35625,15.98125, RGB=0,51,255, THICKEN=.TRUE./

&OBST ID='Lletra B', XB=20.8625,20.925,-4.838897,-4.588897,15.325,16.0125, RGB=0,51,255, THICKEN=.TRUE./

&OBST ID='Lletra B', XB=20.925,20.9875,-4.838897,-4.588897,15.35625,15.98125, RGB=0,51,255, THICKEN=.TRUE./

&HOLE ID='Entrada P6', XB=18.5,21.5,4.0,4.3,15.2,17.4, COLOR='INVISIBLE'/

&HOLE ID='Porta LAB', XB=16.0,17.2,10.05,10.25,15.2,17.4, COLOR='INVISIBLE'/

&HOLE ID='Porta VI', XB=18.0,18.2,8.2,9.4,15.2,17.4/

&HOLE ID='Entrada P6', XB=18.5,21.5,4.0,4.3,18.15,20.35, COLOR='INVISIBLE'/

&HOLE ID='Vestibul', XB=15.0,22.0,4.0,4.3,-0.1,2.65, COLOR='INVISIBLE'/

&VENT ID='Mesh Vent: Mesh01-01 [YMAX]', SURF_ID='OPEN', XB=4.0,23.0,7.0,7.0,-1.0,14.862069, COLOR='INVISIBLE'/

&VENT ID='Mesh Vent: Mesh01-04 [XMIN]', SURF_ID='OPEN', XB=4.0,4.0,-7.0,29.0,14.862069,22.0, COLOR='INVISIBLE'/

&VENT ID='Mesh Vent: Mesh01-04 [YMAX]', SURF_ID='OPEN',

XB=4.0,23.0,29.0,29.0,14.862069,22.0, COLOR='INVISIBLE'/

&VENT ID='Mesh Vent: Mesh01-04 [ZMIN]', SURF_ID='OPEN',

XB=4.0,23.0,7.0,29.0,14.862069,14.862069, COLOR='INVISIBLE'/

&VENT ID='Fire Vent', SURF_ID='Foc', XB=16.5,18.0,27.0,28.0,16.1,16.1/

&SLCF QUANTITY='TEMPERATURE', CELL_CENTERED=.TRUE., ID='TEMPERATURE', PBX=16.5/

&SLCF QUANTITY='VOLUME FRACTION', SPEC_ID='CARBON MONOXIDE', CELL_CENTERED=.TRUE., ID='CO', PBX=16.5/

&SLCF QUANTITY='VELOCITY', VECTOR=.TRUE., CELL_CENTERED=.TRUE., ID='VELOCITY', PBX=16.5/

&SLCF QUANTITY='VELOCITY', VECTOR=.TRUE., ID='VELOCITY', PBX=20.0/

&TAIL /

